GIS

Universität Stuttgart

Satellite Altimetry for Hydrological Purpose

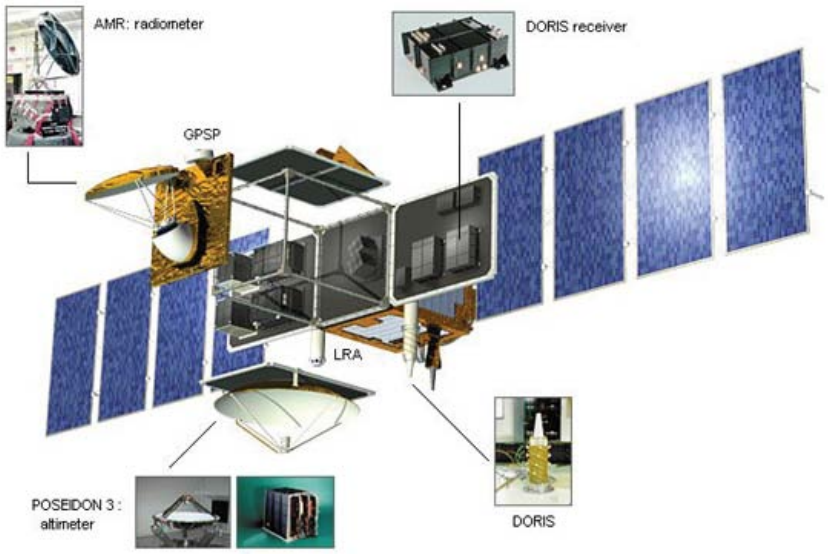

Master Thesis

GEOENGINE

Yuxing LI

October 2011

Supervisors: Prof.Dr.-Ing. Nico Sneeuw

M.Sc. Mohammad J. Tourian

Declaration of thesis

I declare here solemnly that this thesis is a presentation of my original research work. Wherever contributions of others are involved, every effort is made to indicate this clearly, with due reference to the literature, acknowledgement of research and discussions.

Place, Date Signature

ABSTRACT

As a new spatial measuring technic developed in 1970s, altimetry was designed to determine the sea surface height based on spatial technology, electronic technology and microwave technology. It also plays an important role in geodesy and oceanography; meanwhile, it can provide all-weather and repetitious measurements in global region for the studying of variation of SSH, earth gravity field, ocean circulation as well as submarine topography. In addition, real-time data can also be provided for the field of weather forecast, ocean circulation forecast and wave forecast in globally.

Satellite radar altimetry, well known as TOPEX/POSEIDON, JASON, ENVISAT, which have been originally designed to measure global ocean surface height, nowadays, also demonstrated with great potential for applications of inland water body studies.

Therefore, the main task of this study is to analyze and summarize the relevant theory and technology of altimetry waveform, waveform retracking methods based on the investigative research up to now. And above all, data used in this study is Topex geophysical data and sensor data from 1992 until 2002 provided by NASA (http://podaac.jpl.nasa.gov/). The main content of this study are listed as follows:

- ✓ Discuss the theory and process of altimeter waveform, and distinguish the real waveforms from ideal ones.
- ✓ Waveform classification based on different shapes.
- ✓ Automatic waveform filter is designed to move out noisy data.
- ✓ The most popular retracking methods (OCOG, Threshold, 5β) are compared and evaluated with respect to different groups of waveform. And finally an optimal Lake level height is to be generated by sufficient combing all the above retracking methods.
- ✓ Generate time series of Lake level height (from 10Hz data) in selected water bodies; evaluate the result by comparison with in-situ gauge data.

Table of contents

CHAPTER 1

INTRODUCTION

1.1 Introduction

Satellite radar altimetry, which was initially designed for accurate measurements of sea surface height, ocean circulation and sea level, has been demonstrated to be applicable to non-ocean surfaces as well (Zwally, 1989). It has been shown that through the analysis of radar waveforms, the profile of backscattered power and the geophysical information related to the near-surface properties can be derived. In addition, satellite radar altimetry has been used to measure inland water level variation for hydrologic studies (Lee H.K., 2009). Whereas these studies focused on large river basins such as the Amazon, attempts have been made to measure water level change over vegetated wetlands using TOPEX/POSEIDON radar altimetry.

Normally, the radar altimeter over varying terrains differs significantly from that of sea surface, which leads the altimeter's on-board tracker to fail in precisely predicting the range (Zhang, M.M., 2009). Especially when satellite moves from vast ocean surface to inland waters, the accuracy is supposed to be reduced since environment becomes much more complicated. Thus, altimeter range measurement over non-ocean surface must be corrected for the deviation of the real range, this process is called retracking. Retracking is important to enhance the altimeter data accuracy which could be low in small water bodies due to land contaminations in the received signal.

During the past 30 years, scholars around the world have researched quite a lot, focusing on the application of satellite altimetry in inland use (Lee, H.K., Shum C. K., 2010). Here, this study attempts to combine different retracking algorithms together, aims at generating time series of water level height of inland water bodies.

1.2 Motivation

There are hundreds of thousands of lakes in the world. However, it is still unclear how the storage of these water bodies changes and how they behavior with the global change of climate. Thus understanding variations in lake levels plays an important role in studying climate change (Guo J.Y., 2009).

Hydrology is a science dealing with the global water change, which is related to the origin, distribution, volume and properties of water on the earth (Dingman, 2001). Understanding and Modeling of hydrology represent the basis for development and management of water resources. Despite its importance, hydrology has been studied during the past thousands of years, but still hindered by the limitation of traditional hydrological method: in-situ gauge measurement. Clearly, it is not possible and

not enough with only the in-situ gauge because the distribution of water bodies is really vast and discrete. Meanwhile, the stage gauge measurements are only available at limited sites of certain water basins. Thus, satellite remote sensing method seems to be a much more effective solution for hydrologic studies over a large basin or at the global scale with adequate temporal and spatial resolutions (Zhang M.M., 2009).

Figure 1.1 Example of traditional in-situ gauge measurement and satellite altimetry. We can see the limitation of in-situ gauge method, while the advantage of satellite remote sensing is its global water resources measurement and management.

Comparing with traditional in situ gauge measurement, one particular advantage of satellite altimetry is: it provides nearly global coverage measurement, which means, not only inland rivers but also vast oceans could be measured as well.

Even though satellite altimetry was initially designed for vast ocean measurement, aims at overcome the limitation of traditional method. However, based on previous studies (Hwang, C.H., 2004), it also demonstrated great potentials for inland studies with pretty good accuracy, and we all know that inland waters, such as rivers, lakes and wetland, are much more closely linked with humans' daily life comparing with vast oceans. Thus, satellite altimetry provides a new solution to manage and monitor the water resources, which is much faster, convenient and low costing than ever before.

Therefore, in this study, I will investigate and verify the performance of satellite altimetry in inland use. The selected area will be very typical inland water resources, including rivers, lakes and seas.

1.3 Content and purpose

In this study we have analyzed and summarized the relevant theory and technology of altimetry waveform, waveform retracking methods based on the investigative research during the past decades. Furthermore, lots of efforts have been tried to make a sufficient combination of different waveform retracking algorithms optimally, since each method has its own advantage and disadvantage.

In summary, the main content of this study is listed as follows:

(1) Discussion of the structure and content of Topex/Poseidon data.
(2) Discuss the theory and process of altimeter waveform, and analyze the ideal waveform and the real waveform.
(3) Waveforms analysis, including classification based on different shapes, noisy waveform detection and filter.
(4) The most popular retracking methods such as OCOG, Threshold, 5β are compared and evaluated with respect to different groups of waveform. And finally an optimal Lake level height is to be generated combing all the above retracking methods.

CHAPTER 2

TOPEX/POSEIDON OVERVIEW

2.1 Introduction

Since 1973 the first altimetric satellite Skylab was launched, today we already have a big family of satellite altimetry (Figure 2.1 from http://earth.esa.int/, 2010).

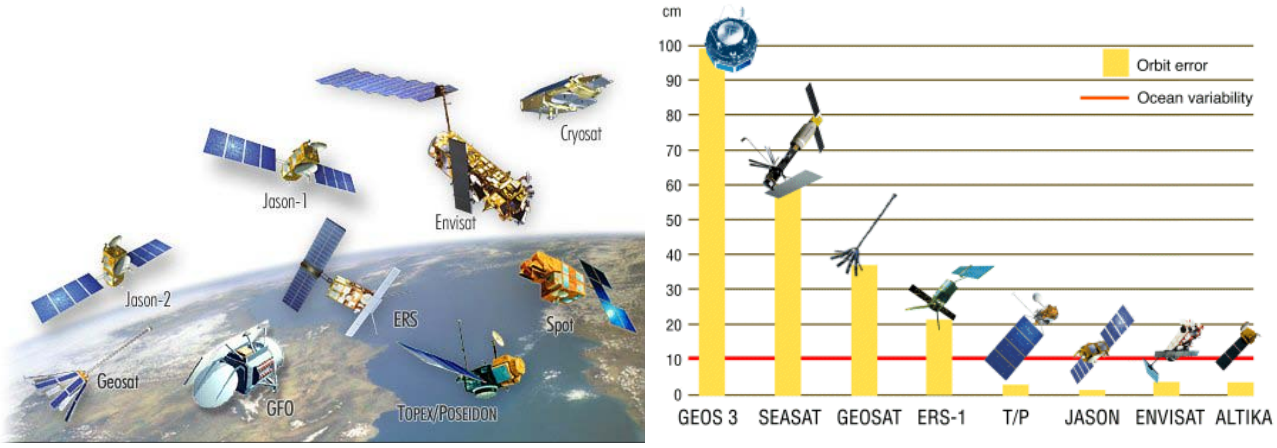

(a) (b)

Figure 2.1 (a) A group of active duty altimetric satellite, including the first altimetric satellite with centimeters accuracy in orbit error, Topex/Poseidon, and the most recent satellite Jason2. (b) Shows the orbit errors of each satellite. In this study, T/P was preferred for the following two reasons: high accurate and long service periods.

TOPEX/POSEIDON was launched on August 10, 1992. It is a joint satellite mission by the United States' National Aeronautics and Space Administration (NASA) and the French Space Agency, Centre National d'Etudes Spatiales (CNES), aims at studying the global circulation from space. The mission uses the technique of satellite altimetry to make precise and accurate observations of sea level for several years, and TOPEX/Poseidon's radar altimeter provided the first continuous global coverage of the surface topography of the oceans.

The major goals of the TOPEX/POSEIDON mission are listed as follows:

(1) Measure the sea level in a way that allows the study of ocean dynamics, including the calculation of the mean and variable surface geostrophic currents and the tides of the world's oceans.

(2) Process, verify and distribute the data in a timely manner, with other geophysical data, to science investigators.

(3) Lay the foundation for a continuing program to provide long-term observations of the oceanic circulation and its variability (Topex/Poseidon Handbook, 1996).

2.2 Satellite Description

The major elements of T/P include the following several elements:

(1) A satellite carrying an altimetric system for measuring the height of the satellite above the sea surface.
(2) A precision orbit determination system for referring the altimetric measurements to geodetic coordinates.
(3) A data analysis and distribution system for processing the satellite data, verifying their accuracy, and making them available to the scientific community.
(4) A principal investigator program designed for scientific studies based on the satellite observations.

2.2.1 Sensors

The science and mission goals are carried out with a satellite carrying six science instruments, four from NASA and two from CNES. They are divided into operational and experimental sensors as follows:

We begin with 4 operational sensors:

(1) Dual-frequency Ku/C band Radar Altimeter (NRA) (NASA)

The NRA, operating at 13.6 GHz (Ku band) and 5.3 GHz (C band) simultaneously, is the primary sensor for the TOPEX/POSEIDON mission. The measurements made at the two frequencies are combined to obtain altimeter height of the satellite above the sea (satellite range), the wind speed, wave height and the ionosphere correction. This instrument is the first space borne altimeter that uses two-channel measurements to compute the effect of ionospheric free electrons in the satellite range measurements. It is redundant except for the microwave transmission unit and the antenna (Topex/Poseidon Handbook, 1996).

(2) Three-frequency TOPEX Microwave Radiometer (TMR) (NASA)

The TMR measures the sea surface microwave brightness temperatures at three frequencies (18 GHz, 21 GHz and 37 GHz) to provide the total water-vapor content in the troposphere along the altimeter beam. The 21 GHz channel is the primary channel for water-vapor measurement. The 18 GHz and 37 GHz channels are used to remove the effects of wind speed and cloud cover, respectively in the water-vapor measurement. TMR data are sent to CNES for processing along with their altimeter data. The measurements are combined to obtain the error in the satellite range measurements caused by pulse delay due to the water vapor (Topex/Poseidon Handbook, 1996).

(3) Laser Retro reflector Array (LRA) (NASA)

The LRA reflects signals from network of 10 to 15 satellite laser tracking stations to calibrate NRA bias and to provide the baseline tracking data for NASA precise orbit determination (Topex/Poseidon Handbook, 1996).

(4) Dual-frequency Doppler tracking system receiver (DORIS) (CNES)

The DORIS system uses a two-channel receiver (1401.25 MHz and 2036.25 MHz) on the satellite to observe the Doppler signals from a network of 40 to 50 ground transmitting stations. It provides all-weather global tracking of the satellite for CNES precise orbit determination and an accurate correction for the influence of the ionosphere on both the Doppler signal and altimeter signals.

Then we will talk about 2 experimental sensors:

The two experimental instruments are intended to demonstrate new technology.

(1) Single frequency Ku band Solid State Altimeter (SSALT) (CNES)

The SSALT, operating at a single frequency of 13.65 GHz (Ku band), will validate the technology of a low-power, light-weight altimeter for future Earth-observing missions. It shares the antenna used by the NRA; thus only one altimeter operates at any given time. Measurements give the same geophysical information as NRA's. However, since this sensor uses a single frequency, an external correction for the ionosphere must be supplied.

(2) Global Positioning System Demonstration Receiver (GPSDR) (NASA)

The GPSDR, operating at 1227.6 MHz and 1575.4 MHz, uses the technique of GPS differential ranging for precise orbit determination.

2.2.2 Orbit

The orbit chosen for the Topex/Poseidon mission is a compromise among a number of conflicting requirements. It provides broad coverage of the ice free oceans (See figure 2.2) as frequently as possible without aliasing the tides to unacceptable frequencies, and it is high enough to ease the precision of the orbit determination process in minimizing the atmospheric drag. We can read T/P orbit parameters from the following table.

Table 2.1 Orbit parameters of Topex/Poseidon

Semi-major axis	7 714.43 km
Eccentricity	0.000095
Inclination	66.04°
Argument of periapsis	90°
Reference altitude	1336 km
Nodal period	6 745.72 s
Repeat period	9.9156 days
Equatorial cross-track separation	315 km
Ground track control band	+ 1 km
Acute angle at Equator crossings	39.5°
Orbital speed	7.2 km/s
Ground track speed	5.8 km/s
Number of revolutions within a cycle	127
Service Period	1992−2006

In the following figure, it shows one complete cycle of orbit, from which we can have a preview about the global coverage of Topex/Poseidon.

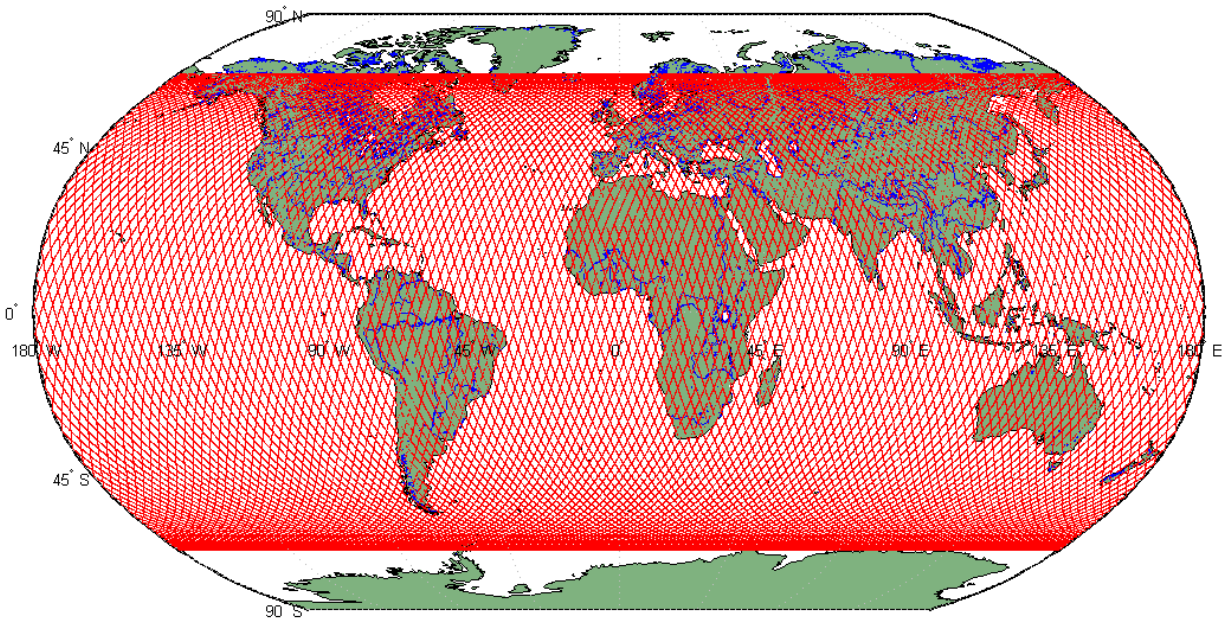

Figure 2.2 One complete cycle of Topex/Poseidon, within 10 days, all together there are 127 revolutions. And the distance between neighboring cross track at equator is 315 km.

2.2.3 Accuracy

Each measurement of sea level shall have a precision of +2.4 cm and an accuracy of +14 cm (standard deviation) for typical oceanic conditions, with small geographically correlated errors (Zhang M.M., 2009). In this context, precision is the ability to determine changes in sea level over distances of 20 km, and accuracy is the uncertainty of each measurement of sea level when expressed in geocentric coordinates (WGS 84).

2.3 Topex/Poseidon Data

Radar altimetry from space consists of vertical range measurements between the satellite and water level. Difference between the satellite altitude above a reference surface (usually a conventional ellipsoid), determined through precise orbit computation, and satellite-water surface distance, and provides measurements of water level above the reference surface. Placed onto a repeat orbit, the altimeter satellite flies over a given region at regular time intervals (called the orbital cycle), during which a complete coverage of the Earth is performed. Here we use altimetry data from the Topex/Poseidon (T/P) satellite (launched in August1992) to investigate the capability of the altimetric technique to monitor water levels in large hydrographic basins. The temporal resolution of the T/P data is 9.915 days (the duration of an orbital cycle); its ground track coverage is 315km in equatorial regions (NASA). Although not as dense as for the ERS-1/2 coverage (about 4 times denser), the existing T/P data base has the advantage of providing directly altimetric height measurements over land, unlike the ERS-1/2 missions for which only waveforms are available. We have analyzed eight years of Topex/Poseidon altimetry data from January 1993 to December 2000, using the most upgraded GDRs (Geophysical Data Records) made available by the JPL.

The GDRs contain range values derived from averaged radar echoes at 100 ms and 1 s interval, which corresponds to along-track ground spacing of 580 m and 5.8 km, respectively. We used both data sets. In addition to the altimetric heights and radial orbit component, the data set includes a series of environmental and geophysical corrections. Over open ocean these corrections include: ionosphere correction, dry and wet troposphere correction, solid Earth, ocean and pole tides, ocean tide loading, inverted barometer effect and sea state bias. Models for these corrections have been improved continuously along the T/P life-time to increase the precision of sea surface heights for open ocean studies, which is currently at the 1-cm level for a single measurement.

The TOPEX/POSEIDON GDR (Geophysical Data Record) contains global coverage altimeter data. The dataset contains measurements from two altimeters, a NASA dual frequency (Ku and C band) instrument similar to the Geosat altimeter, and a French space agency (CNES) instrument which is a proof-of-concept solid-state altimeter (Ku band). It also contains Sea Surface Height (SSH), significant wave height, ionosphere correction, tides and other geophysical corrections. It is emphasized that this product is considered research data because of the form and content of the data. The data consist entirely of files comprising headers and data records which contain over a hundred parameters for each second. It is swath data and there are no images. This dataset is formatted as big-endian binary. The data are arranged in 10 day cycles that are separated into 254 passes, each about 56 minutes (*PO.DAAC*).

2.3.1 Altimeter Range

An important data of the MGDR (Merged Geophysical Data Record) are the altimeter ranges. An altimeter operates by sending out a short pulse of radiation and measuring the time required for the pulse to return from the sea surface. This measurement, called the altimeter range, gives the height of the instrument above the sea surface, provided that the velocity of the propagation of the pulse and the precise arrival time are known. The 1 Hz value of range is calculated at mid-frame time (A frame is one full cycle of the instrument, about 0.98 seconds long, and corresponds to one data record). This is derived from the 10 per frame range differences from the one per frame range. The reported range is already corrected for instrument effects (Birkett C.M., 2001).

In practice, the range must be corrected for the atmosphere through which the radar pulse passes and the nature of the reflecting sea surface. Recall all range corrections are defined so they should be added to the range.

The corrected range is given by:

$$\begin{aligned}\text{Corrected Range} = \text{Range} &+ \text{wet troposphere correction} \\ &+ \text{dry troposphere correction} \\ &+ \text{ionosphere correction} \\ &+ \text{electromagnetic bias}\end{aligned} \tag{2.1}$$

As to the above mentioned corrections, they will be discussed later in section 2.4.

2.3.2 Sea Surface Height

Sea surface height (SSH) is the height of the sea surface above the reference ellipsoid. It is calculated by subtracting the corrected range (see section 2.3.1) from the Altitude:

$$\text{SSH} = \text{Altitude} - \text{Corrected Range} \tag{2.2}$$

Where corrected range is defined above in section 2.3.1; Altitude data could be chosen from either NASA orbit or CNES orbit. The two orbits have comparable precisions. Both are given regardless of which altimeter is operating.

2.3.3 Geoid

The geoid is an equipotential surface of the Earth's gravity field that is closely associated with the location of the mean sea surface (Seeber G., 2003). The reference ellipsoid is a bi-axial ellipsoid of revolution. The center of the ellipsoid is ideally at the center of mass of the Earth although the center is usually placed at the origin of the reference frame in which a satellite orbit is calculated and tracking station positions given. The separation between the geoid and the reference ellipsoid is the geoid undulation (http://earth.eo.esa.int).

The geoid undulation, over the entire Earth, has a root mean square value of 30.6 m with extreme values of approximately 83 m and -106 m (Vivien T., 2001). Although the geoid undulations are primarily long wavelength phenomena, high frequency changes in the geoid undulation are seen over seamounts, trenches, ridges, etc., in the oceans. The calculation of a high resolution geoid requires high resolution surface gravity data in the region of interest as well as a potential coefficient model that can be used to define the long and medium wavelengths of the Earth's gravitational field. If no surface gravity data is used the highest degree expansion of the Earth's gravitational potential is desired. Currently such expansions can be done to degree 360 and in some cases higher (Topex/Poseidon Handbook, 1996).

Since the geoid undulations have been computed from an expansion to degree 360, the resolution of the undulations will be on the order of 50 km. In addition the estimation of the high frequency part of the potential coefficient model (OSU91A) was primarily based, in the ocean areas on Geosat ERM data so that high frequency signal between the Geosat tracks may not be represented in the geoid undulation. One should also note that the effect of neglected information above degree 360 is approximately, 24 cm. which may be larger in ocean areas of high frequency signal and lower in benign areas. The approximate standard deviation, in the ocean areas of the geoid undulation computed from the JGM3/OSU91A model is approximately 26 cm (Vivien T., 2001). Improvements continue to be sought in the estimation of the gravitational potential of the Earth. Developments now underway will lead to substantial improvements in our knowledge of the geoid at all wavelengths.

2.3.4 Flagging/Editing Data

In practice, there is no consensus on data editing for TOPEX/POSEIDON data. As we will see, data editing is applied in order to remove some less accurate data. One may develop as a result of on-going research but for now the user must give careful attention to which data records to include or exclude.

For inland use, the formula we will be using is:

(1) The RMS of various quantities

(2) The number of points averaged into a compressed SSH, AGC, Sigma0, or SWH

(3) Values being outside of "normal" limits where processing flag limits were set rather wide (For example, sigma0 is flagged only > 40 dB, but values above approximately 16 to 20 dB indicate anomalous ocean returns). Table 2.2 and Table 2.3 show the data editing of T/P applied in my study.

Table 2.2 Data Editing when Topex Altimeter On

Topex Altimeter On				
Flagging	Restrictions		Flagging	Restrictions
Nval_H_Alt >= 6	Sufficient 10/second measurements		SWH_K <= 1500	SWH in reasonable range
Geo_Bad_1, bit 1 = 0	not land		Geo_Bad_1, bit 3 = 0	not ice
Geo_Bad_1, bit 2 = 0	TMR over water		Geo_Bad_2, bit 0 = 0	TMR not excess liquid water
Geo_Bad_2, bits 1, 2 <= 3	Tide Model quality good		Iono_Corr! = Default Value	dual frequency ionosphere correction exists
Sat_Alt! = Default Value	orbit height exists		EMB_Gaspar! = Default Value	EM Bias correction exists
Dry_Corr! = Default Value	dry correction exists		H_Pol! = Default Value	Pole Tide exists

Table 2.3 Data Editing when Poseidon Altimeter On

Poseidon Altimeter On				
Flagging	Restrictions		Flagging	Restrictions
Nval_H_Alt >= 15	Sufficient 10/second measurements		SWH_K <= 1500	SWH in reasonable range
Geo_Bad_1, bit 1 = 0	not land		Geo_Bad_1, bit 3 = 0	not ice
Geo_Bad_1, bit 2 = 0	TMR over water		Geo_Bad_2, bit 0 = 0	TMR not excess liquid water
Geo_Bad_2, bits 1, 2 <= 3	Tide Model quality good		Iono_Dor_Bad <= 3	Doris ionosphere exists and is good
Sat_Alt! = Default Value	orbit height exists		EMB_Gaspar! = Default Value	EM Bias correction exists
Dry_Corr! = Default Value	dry correction exists		H_Pol! = Default Value	Pole Tide exists
H_Set! = Default Value	Solid Earth Tide exists		RMS_H_Alt <= 175	1 sec average not noisy

If analysis is to be done near land, it may be necessary to ignore not only Geo_Bad_1 bit 0 (deep water), but also bit 2 (TMR land) and Geo_Bad_2 either bits 1, 2 or 3, 4 - ocean tide. Depending on which tide model is used. Unless the user has a precise land map against which to check the locations, Geo_Bad_1 bit 1 (altimeter land) should be checked as other flags may not change immediately for some water to land transitions.

The above flags have to be considered at the very beginning, besides, in my study, the following factors (Table 2.4) have also been added into program aims at removing certain so called “Bad” data to improve the quality of observations in use.

Table 2.4 Further Data Editing

T/P Data Editing				
Flagging	Restrictions		Flagging	Restrictions
Nval_H_Alt >= 5	Sufficient number of valid observations		is_bounded(0,rms_h_alt,0.1)	Good quality of range
is_bounded(-2.5,dry_corr,-1.9)	Proper dry troposphere correction		is_bounded(-0.500,wet_h_rad,-0.001)	Proper wet troposphere correction
is_bounded(-0.4,iono_cor,0.04)	Proper ionosphere correction		is_bounded(7,sigma0_k, 30)	Proper wet troposphere correction
is_bounded(-1,h_set,1)	Proper wet troposphere correction		is_bounded(-0.150,h_pol,0.150)	Proper wet troposphere correction

2.4 Geophysical Corrections

The atmosphere and ionosphere slow the velocity of radio pulses at a rate proportional to the total mass of the atmosphere, the mass of water vapor in the atmosphere, and the number of free electrons in the ionosphere. In addition, radio pulses do not reflect from the mean sea level but from a level that depends on wave height and wind speed. While not large, the errors due to these processes cannot be ignored and must be removed.

It should be noted here that the height parameter is based on the utilization of the NASA T/P orbit and the radio positioning integrated by satellite (DORIS) ionosphere range correction. In addition, no corrections are applied to account for the wet tropospheric range correction, various surface slope and tidal effects (Birkett C.M., 2001).

2.4.1 Troposphere (dry and wet)

The propagation velocity of a radio pulse is slowed by the "dry" gasses and the quantity of water vapor in the Earth's troposphere. The "dry" gas contribution is nearly constant and produces height

errors of approximately -2.3 m. The water vapor in the troposphere is quite variable and unpredictable and produces a height calculation error of -6 cm to -40 cm. However, these effects can be measured or modeled as discussed below (Lee H.K., 2008).

The gases in the troposphere contribute to the index of refraction. Its contribution depends on density and temperature (Satellite altimetry and earth sciences, page 38). When hydrostatic equilibrium and the ideal gas law are assumed, the vertically integrated range delay is a function only of the surface pressure. The dry meteorological tropospheric range correction is equal to the surface pressure multiplied by -2.27 mm/m. There is no straight forward way of measuring the nadir surface pressure from a satellite, so it is determined from model assimilated weather data from the European Center for Medium Range Weather Forecasting (ECMWF). The uncertainty on the dry tropospheric correction is about 0.7cm (Lee H.K., 2010).

The amount of water vapor present along the path length contributes to the index of refraction of the Earth's atmosphere. Its contribution can be estimated by measuring the atmospheric brightness near the water vapor line at 22.2356 GHz and providing suitable removal of the background. The TOPEX Microwave Radiometer (TMR) measures the brightness temperatures in the nadir path at 18, 21 and 37 GHz: the water vapor signal is sensed by the 21 GHz channel, while the 18 GHz removes the surface emission (wind speed influence), and the 37 GHz removes other atmospheric contributions (cloud cover influence). Measurements are combined to obtain the error in the satellite range measurement due to water vapor effect. The uncertainty is +1.2 cm (Lee H.K., 2008).

Elsewhere, the meteorological model calculates also a value of the wet tropospheric delay which is placed on the MGDR as a backup to the TMR. This backup will prove useful when sun glint, land contamination, or anomalous sensor behavior makes the TMR data unusable.

2.4.2 Ionosphere

At the frequencies used by the TOPEX/POSEIDON altimeters, the propagation velocity of a radio pulse is slowed by an amount proportional to the number of free electrons of the Earth's ionosphere. The retardation of velocity is inversely proportional to frequency squared. For instance, it causes the altimeter to slightly over-estimate the range to the sea surface by typically 0.2 to 20 cm at 13.6 GHz. The amount varies from day to night (very few free electrons at night), from summer to winter (fewer during the summer), and as a function of the solar cycle (fewer during solar minimum).

Because this effect is dispersive, measurement of the range at two frequencies allows it to be estimated. Thus it is computed from the TOPEX data with an expected accuracy of 0.5cm and from DORIS measurements with accuracy of 2 cm. The first term is only valid for TOPEX data and the second term for TOPEX and POSEIDON data. The average of TOPEX versus DORIS difference is nearly 1cm with an RMS of 2cm (depending on the local time of the cycle). As a backup, the Bent model correction is also placed on the MGDR (Lee H.K., 2010).

While this 2 cm RMS difference is small viewed globally, there are large differences in some regions. The main areas are the western Pacific due to lack of DORIS coverage and the equatorial Atlantic due to insufficient geomagnetic modeling. The sub solar point is another area of discrepancy due to the peak of the electron content.

2.4.3 Tide

Tides are obviously a significant contributor to the observed sea surface height. While they are of interest in themselves, they have more energy than all other time-varying ocean signals. Since they are highly predictable, they are removed from the data in order to study ocean circulation. The TOPEX/POSEIDON orbit was specifically selected (inclination and altitude) so that diurnal and semidiurnal tides would not be aliased to low frequencies. There are several contributions to the tidal effect: the elastic ocean tide, the solid earth tide and the pole tide. The elastic ocean tide is the sum of the pure ocean tide (equilibrium and non-equilibrium tides) and the loading tide. The pole tide is due to variations in the earth's rotation and is unrelated to lunisolar forcing. Ocean tides are one of the most fascinating natural events in the world (Le Provost, 2001).

However, in this study, correction to tide was neglected since lake tides over majority small inland lakes are believed to be small (only cm level) (Hwang C.W., 2010).

2.5 Principle of Satellite Radar Altimetry

Satellite radar altimetry is a revolution technology to measure the height and the shape of the sea surface globally from space. It was designed and has been used to observe global oceanic topography and its change. Figure 3.1 shows the principle of satellite altimetry in general.

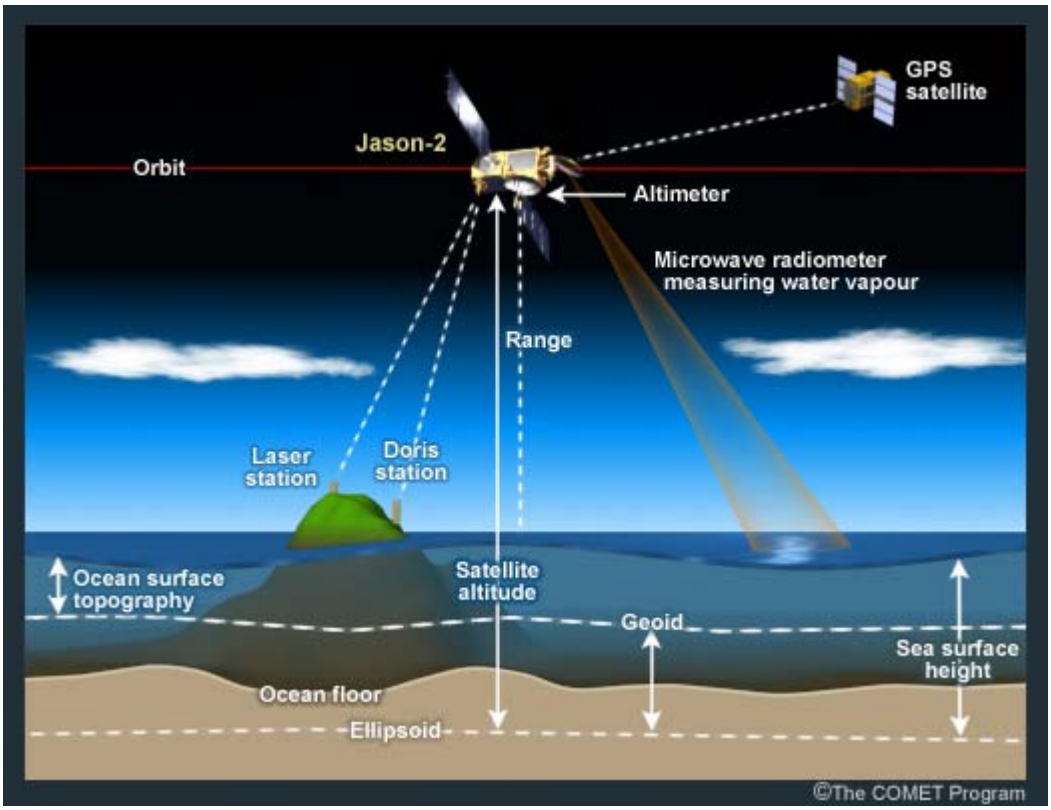

Figure 3.1 The principle of satellite altimetry. With the help of GPS, orbit errors of T/P could be determined very precisely within 2 cm. Meanwhile, range could be calculated by two way travelling time of pulse between the satellite and sea surface, finally, altitude minus range, sea surface height could be derived.

The observation principle of satellite altimetry is to measure the two-way travelling time t of electromagnetic pulse from satellite to instant sea surface, and then the range can be derived as

$$R = \frac{ct}{2} \tag{2.3}$$

Here, c is the speed of light in free space.

This instant range measurement must be corrected for the instrument、the atmospheric propagation and the geophysical surface height variations, and then we got the so called “Corrected Range”, as has been mentioned in section 2.3.1.

Finally, sea surface height (SSH) is the height of the sea surface above the reference ellipsoid. It is calculated by subtracting the corrected range (see above) from the Altitude:

$$\text{SSH} = \text{Altitude} - \text{Corrected Range} \tag{2.4}$$

Even though the principle of satellite altimetry seems to be oversimplified, however, it is a little bit difficult to understand how it works exactly behind.

CHAPTER 3

SATELLITE ALTIMETRY WAVEFORM

3.1 Waveform

The basic concept of satellite altimetry could be described as follows: when satellite travels above the water body, the altimeter transmits a short pulse of microwave radiation with pre-defined power toward the target surface. The pulse interacts with the rough surface and part of the incident radiation reflects back to the altimeter.

In the field of satellite altimetry, waveform is actually a curve which shows the power reflected back to the altimeter.

3.1.1 Two way travel of signal

The basic measurement from satellite altimetry is the ratio of the power of pulse received at the antenna and the power transmitted from the antenna. After the electromagnetic radiation is transmitted from the satellite, it's attenuated while it went through the atmosphere, then it reaches the water surface (See figure 3.2). Some of the pulses are reflected and some are absorbed by the water. On the way back to satellite, the power is attenuated again by the atmosphere and received by the satellite.

To study the waveform, here we pay attention to the following specific process, as the incident pulse strikes the surface; it illuminates a circular region that increases linearly with time. Correspondingly, a linear increase in the leading edge of the return waveform occurs. After the trailing edge of the pulse has intersected the surface, the region back-scattering energy to the satellite becomes an expanding annulus of constant area. At this point, the return waveform has reached its peak and then begins to trail off due to the reduction of the off-nadir scattering by the altimeter's antenna pattern.

And in the following figure we will see in detail the procedure that a waveform is generated, and how the travelling time is counted as well.

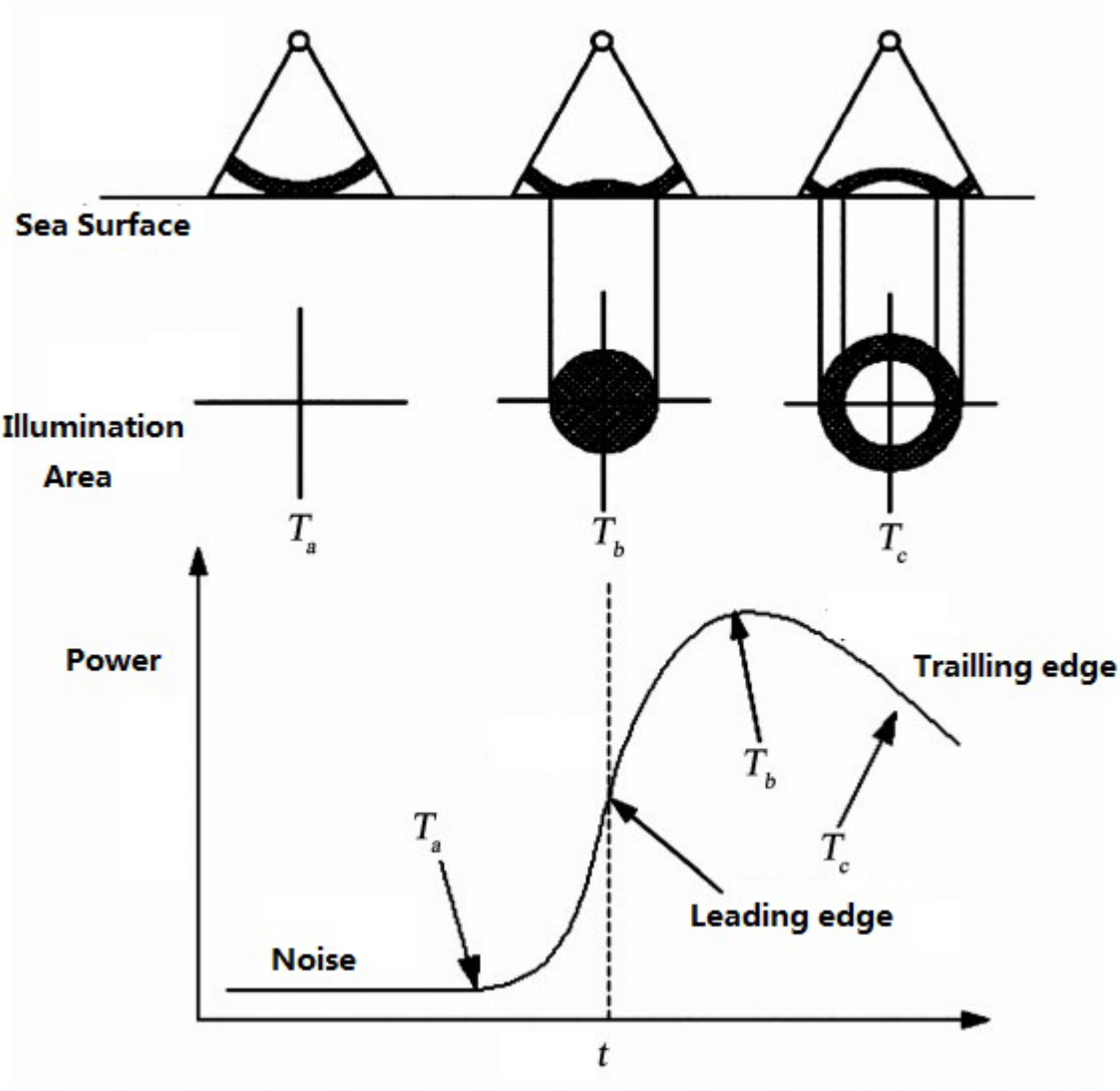

Figure 3.2 Two ways travelling of signal between the satellite and water surface. At time T_a signal reaches the water surface, from T_a to T_b power keeps increasing, at T_b power becomes maximum value. After T_b, signal is reflected back to satellite. And the waveform below shows actually the power reaches and reflected from the water surface. In this case, the sea surface is ideal flat, thus, such standard waveform is also named as "Brown Model" (Vivien E., 2007).

The one way travelling time of signal is actually the mid-point of leading edge (Lee H.K., Shum C.K., 2006).

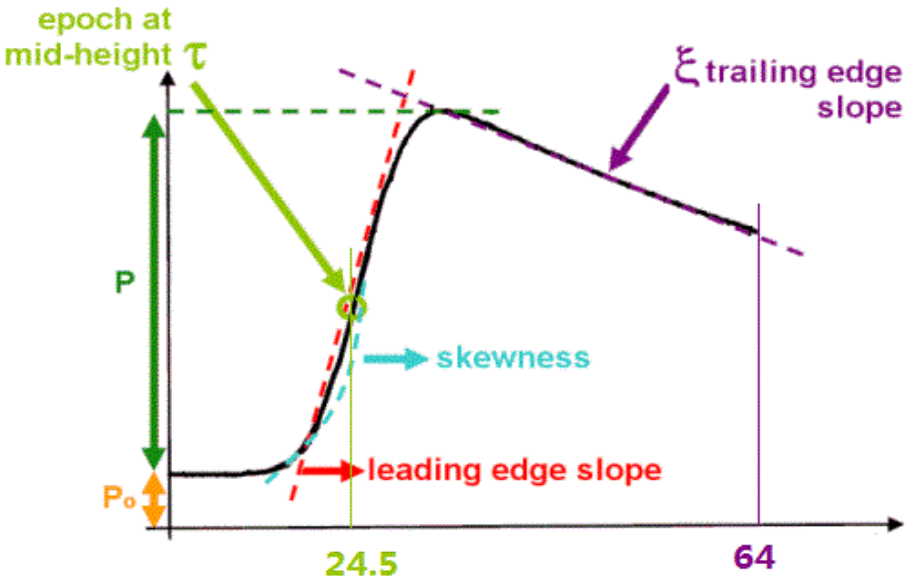

Figure 3.3 An example of standard waveform generated from T/P altimeter, in which the whole waveform is divided into 64 samples, better known as "64 bins" waveform. Here we can see that a waveform is composed by several components like amplitude, leading edge slope and trailing edge slope, among them the most important part is the leading edge slope, in fact, the corresponding bin at the mid-point of leading edge is actually the one way travelling time of signal.

However, in normal case, the reflection surface is not always as ideal as expected, especially when it comes to inland water, environment becomes complicated. Radar echoes over land surfaces are hampered by interfering reflections due to water, vegetation canopy and rough topography. As a consequence, waveforms (e.g., the power distribution of the radar echo within the range window) may not have the simple broad-peaked shape seen over ocean surfaces, but can be complex, multi-peaked, preventing from precise determination of the altimetric height (Oliveira C., 2001).

Therefore, certain waveforms might become so noisy that we cannot derive any useful information from them at all. Thus, the so called "Noisy waveform" is supposed to be filtered out before waveform retracking (As will be explained in section 3.1.2).

3.1.2 Waveform Retracking

Although satellite altimetry was initially designed for ocean studies, however, when it comes to non-ocean surface, the performance of radar altimeters differs significantly from that of ocean surface, thus, the reflected waveform from non-ocean surface turns to be not standard as before, due to several possible reasons: complicated topography, coverage of forest or even the depth of water body itself, etc.

As a result, when we study satellite altimetry for inland water use, one problem is the satellite on-board tracker may fail in precisely predicting the range. In detail, since the waveform in non-ocean surface becomes noisy, therefore the position of leading edge differs depending on the topography below, and for such situation, it is not difficult to imagine that the mid-point of leading edge differs as well. The pre-defined leading edge of T/P was initially designed to 24.5, which means T/P still believes the mid-point of leading edge should be 24.5, so the range computed by T/P is not correct.

Here it should be mentioned that the 64 bin waveforms are averaged into 128 bin waveforms by certain rules, which could be summarized in table 3.1.

Table 3.1 128 sample waveforms averaged into 64 sample waveform

128 sample waveform	64 sample waveform	Rule	Sampling rate
1-16	1-8	Averaged by two	6.25 ns
17-48	9-40	One to One	3.125 ns
49-64	41-48	Averaged by two	6.25 ns
65-128	49-64	Averaged by four	12.5 ns

Since the tracking point of 128 sampling waveform is 32.5, so we can easily transform it into 64 sampling waveform:

$$G0=16/2+16.5=24.5 \tag{3.1}$$

That is why we have to find out the true position of waveform leading edge, and make certain corrections on to the range given by T/P itself, and this process is named as waveform retracking. Here in Figure 3.4, it shows a group of typical waveforms from inland water surface.

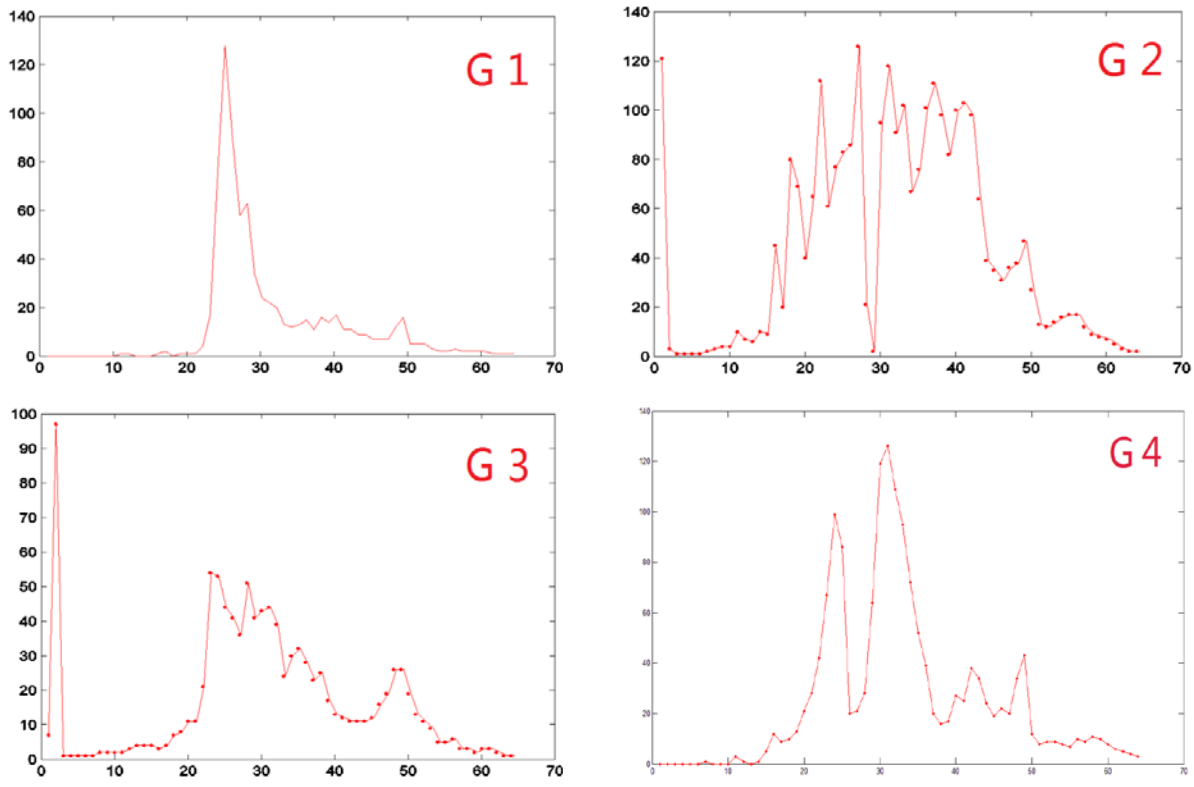

Figure 3.4 A group of typical waveforms from inland water body. Waveform in Group (G1) could be regarded as ideal waveforms from inland water body. (G2) shows multi-peak noisy waveforms due to surrounded buildings or vegetation. (G3) stands for waveforms with weak power, during the two way path, signal might be absorbed or reflected in all directions, and thus the received power by satellite is low. (G4) shows double peak waveforms, which might come from shallow water surface, in which signal is reflected from both the surface and bottom of the water basin.

3.2 Waveform retracking method

The waveform retracking method is mainly used to calculate the offset between the practical middle point of waveform leading edge and the designed gate, based on which the retracked distance correction can be computed.

There are several retracking methods commonly used at present, they are:

(1) Off Center of Gravity (OCOG).
(2) 5β Method.
(3) Threshold method.

3.2.1 OCOG (Off-Center of Gravity) Algorithm

The OCOG algorithm was developed as an empirical technique to produce ice sheet data products from ERS-1/2 radar altimetry, which is a simple waveform retracking method based on the statistical characteristics of waveforms. It estimates the amplitude of the waveform and uses this to threshold retrack the leading edge (Bamber J., 1994).

In detail, it calculated the center of gravity of a rectangular box and the amplitude is two times the height of the center of gravity. The squares of the sample values are used to reduce the effect of low amplitude samples in front of the leading edge (See detail in figure 3.5).

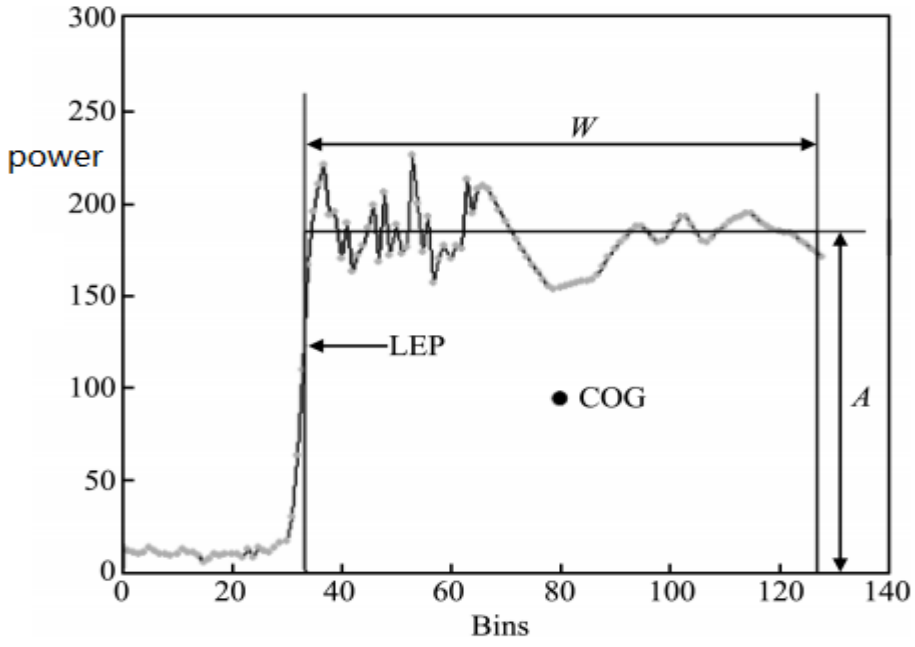

Figure 3.5 Schematic diagram of the OCOG method (GUO Jin-Yun, 2010).

The equations of OCOG are given as:

$$A = \sqrt{\sum_{i=1+n}^{N-n} P_i^4(t) / \sum_{i=1+n}^{N-n} P_i^2(t)} \tag{3.2}$$

$$W = \left(\sum_{i=1+n}^{N-n} P_i^2(t) \right)^2 / \sum_{i=1+n}^{N-n} P_i^4(t) \tag{3.3}$$

$$COG = \frac{\sum_{i=1+n}^{N-n} i \cdot P_i^2(t)}{\sum_{i=1+n}^{N-n} P_i^2(t)} \tag{3.4}$$

where N is the total gate number; n is the number of eliminated gate in the starting and ending of waveform; $P_i(t)$ is the power of the $i\text{-}th$ gate; A is the amplitude; W is the width; COG is the center of gravity of waveform; LEP is the middle point of leading edge.

In addition, the waveform samples 45-50 are exclude to avoid the leakage effects of T/P waveforms (Hayne, 1994).

Finally, the leading edge position is given by:

$$LEP = COG - W / 2 \tag{3.5}$$

Here it should be mentioned that, in most case, OCOG method is used to provide initial values for other algorithms such as 5β and threshold methods, which will be discussed in the following sections.

3.2.2 5β Parametric Fitting Algorithm

The Beta-5 parametric algorithm was initially put forward by Martin in 1983 from the National Aeronautics and Space Administration, USA (NASA). The method uses a relevant parametric function to fit the altimetry waveform based on the Brown mean impulse echo model. In my study, I choose 5 parameters to fit the waveforms.

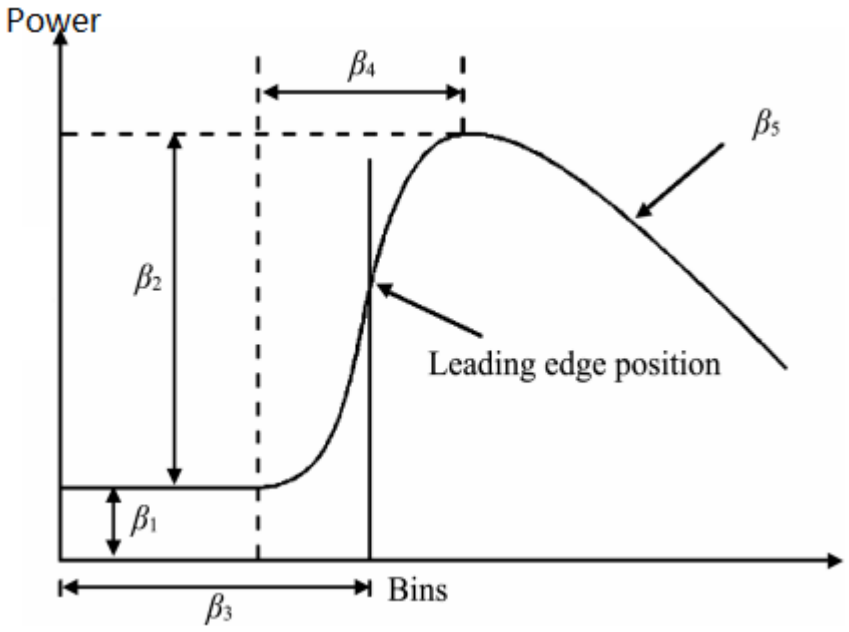

Figure 3.6 Schematic diagram of the 5β method. β_1 is the thermal noise of the waveform to measure the background noise, β_2 is the waveform amplitude which could indicate the surface properties with different reflectivity, β_3 is the mid-point of leading edge which corresponds to the two-way travel time used to compute the altimeter range, β_4 is the slope of the leading edge which is related to significant wave height, β_5 is the slope of ramping edge.

β Parameter can be estimated by the iterative calculation based on good initial values with the least squares adjustment or the maximum likelihood estimator. The 5-βparametric method is mainly used to process the complex waveform returned from the single reflecting surface , better known as "Brown model" waveform. If the waveform is present like a spike, the 5-β parametric algorithm may be non-convergent in the iterative procedure and cannot give the right results.

The non-linear beta-5 parameter equations are given as follows:

$$y(t) = \beta_1 + \beta_2(1+\beta_2 Q)P(\frac{t-\beta_3}{\beta_4}) \tag{3.6}$$

Where

$$Q = \begin{cases} 0 & t < \beta_3 + 0.5\beta_4 \\ t-(\beta_3+0.5\beta_4) & t \geq \beta_3 + 0.5\beta_4 \end{cases} \tag{3.7}$$

$$P(x) = \int_{-\infty}^{x} \frac{1}{\sqrt{2\pi}} \exp(\frac{-q^2}{2}) dq \tag{3.8}$$

$y(t)$: The sampling power at time t.

$P(x)$: The error function.

Q : A linear function to fit the gradual attenuation echo wave in the ramping edge.

Here it should be mentioned that the above equation should be linearized as:

$$\Delta y = AW\Delta x \tag{3.9}$$

$$\Delta y = [y_1 - y_1^0, y_2 - y_2^0, \cdots, y_n - y_n^0]^T \tag{3.10}$$

$$A = \begin{bmatrix} \frac{\partial y_1}{\partial \beta_1} & \frac{\partial y_1}{\partial \beta_2} & \frac{\partial y_1}{\partial \beta_3} & \frac{\partial y_1}{\partial \beta_4} & \frac{\partial y_1}{\partial \beta_5} \\ \vdots & \vdots & & \vdots\ \vdots\ \vdots & \\ \frac{\partial y_n}{\partial \beta_1} & \frac{\partial y_n}{\partial \beta_2} & \frac{\partial y_n}{\partial \beta_3} & \frac{\partial y_n}{\partial \beta_4} & \frac{\partial y_n}{\partial \beta_5} \end{bmatrix} \tag{3.11}$$

$$\Delta x = [\beta_1 - \beta_1^0, \beta_2 - \beta_2^0, \beta_3 - \beta_3^0, \beta_4 - \beta_4^0, \beta_5 - \beta_5^0]^T \tag{3.12}$$

Since the adjustment is an iteration process, so the initial values for 5 parameters should be estimated at the very beginning (the choice of 5 initial parameters might be various), in my study, they are:

$$\begin{aligned} &\beta_1^0 = 2 \\ &\beta_2^0 = A_0 \text{ (From OCOG)} \\ &\beta_3^0 = LEP \text{ (From OCOG)} \\ &\beta_4^0 = 3.5 \\ &\beta_5^0 = -0.02 \end{aligned} \tag{3.13}$$

W is the weight matrix, which should be carefully chose, and in my study, considering that the leading edge is the most important part of the whole waveform, thus I put more weight onto it.

$$\begin{aligned} &W_N = 1; \quad N = 1 \sim \text{int}(LEP - 3) \\ &W_N = 10; \ N = \text{int}(LEP - 3) + 1 \sim \text{int}(LEP - 1) + 3 \\ &W_N = 1; \quad N = \text{int}(LEP - 1) + 4 \sim 64 \end{aligned} \tag{3.14}$$

3.2.3 Threshold Algorithm

The threshold retracking algorithm was primarily developed to measure ice sheet elevation change (Davis, 1997). The threshold Level should be determined based on the amplitude and the maximum waveform power calculated with OCOG. The retracked point can be obtained to linearly interpolate the neighboring samples close to the intersecting threshold between the threshold level and the leading edge. The threshold method is a statistical method and not of physical characteristics. The method can give more precise retracking gate than OCOG (Guo J.Y., 2010).

Normally, for water body studies, we use 50% Threshold level (Guo J.Y., 2010).

The corresponding equations are:

$$P_N = \frac{\sum_{i=1}^{5} P_i}{5} \tag{3.15}$$

$$T_l = (A - P_N) \cdot Th + P_N \tag{3.16}$$

And finally we can compute the mid-point of leading edge:

$$G_r = G_k - 1 + \frac{T_l - P_{k-1}}{P_k - P_{k-1}} \tag{3.17}$$

P_i : Power of $i\text{-}th$ gates.

P_k : Power of $k\text{-}th$ gates.

P_N : The average power of former 5 gates.

Th : The threshold level, here 50%.

G_k : The $k\text{-}th$ gate whose power is more than T_l.

G_r : The middle point of leading edge.

3.2.4 Retracking Distance Correction

After retracking waveforms, the middle point of leading edge can be determined. According to the pre-given gate and the light velocity, the retracking distance correction d_r is:

$$d_r = \frac{c \cdot \Delta Ga}{2} \cdot (G_r - G_0) \tag{3.18}$$

Where ΔGa =3.125 ns is the time interval for one gate; c is the light velocity, c =299792458 m/s; G_r is the middle point of leading edge; and G_0 is the pre-given gate.

Chapter 4

INLAND WATER BODY APPLICATIONS

4.1 Introduction

Inland waters, which connect ocean, wetlands, and land region, play an important role in ecology and environments in inland regions. Inland water bodies not only provide habitat for thousands of aquatic/terrestrial plant and animal species but also control floods by holding water like a sponge and reducing the velocity of storm water. Human activities have many negative impacts on the use of water, which have become one major contributing factor to the water loss and pollution.

The ability to quantitatively measure accurate inland water level changes is critical for ecology and natural hazards mitigation, aim at better understanding and management of water resources. Hence, satellite remote sensing can provide useful measurements to monitor the water level variation over those regions. In addition, satellite radar altimetry has been used to measure inland water level variation over large river basins (Birkett 1998; Alsdorf et al. 2001; Birkett et al. 2002; Maheu et al. 2003; Frappart et al. 2006).

In this study, decadal (1992–2002) TOPEX/POSEIDON data are used to measure water level changes over selected water bodies. We spatially averaged 10-Hz data over a distance corresponding to the intersection between the satellite ground track and the water body, which has an along-track ground spacing of ～660 m (the nominal pulse-limited radar altimetry footprint is a few km), and leads us to obtain much finer along-track spatial sampling comparing with 1 Hz data. The feasibility of applying optimal retracking correction is also demonstrated via validations with in situ river gauge data, whereas previous studies (Birkett 1998; Alsdorf 2001; Birkett 2002; Maheu 2003) considered radar returns from nominal tracking mode contained in TOPEX Geophysical Data Records (GDRs) adequate.

4.2 Target Selection

In this study, places of interest are given to several hot areas in recent research. They are Huron Lake in North American (See Figure 4.1), Aral Sea in Mid Asian (See Figure 4.2 and 4.3) and Amazon Basins (See Figure 4.5).

4.2.1 Huron lake

Lake Huron is one of the five Great Lakes of North America (See figure 4.2). Hydrologically, it comprises the larger portion of Lake Michigan-Huron. It is bounded on the east by the Canadian province of Ontario and on the west by the state of Michigan in the United States. The name of the lake is derived from early French explorers who named it for the Huron people inhabiting the region. Lake Huron is the second largest of the Great Lakes, with a surface area of 59,596 km2. The surface of Lake Huron is 176 m above sea level. The lake's average depth is 59 m, while the maximum depth is 229 m.

Figure 4.1 Huron Lake (http://zh.wikipedia.org/wiki/File:Great_Lakes_Lake_Huron.png, 2005)

4.2.2 Aral Sea

(A)

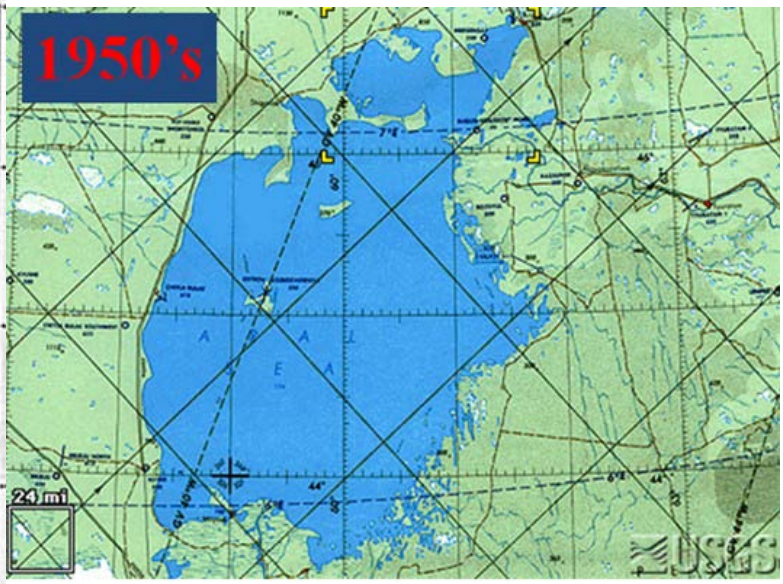

(B)

Figure 4.2 Two maps of Aral Sea at 1850 and 1950 respectively, obviously, during the given 100 years, it seems that not too much change was taken place in Aral Sea. (http://en.wikipedia.org/wiki/Aral_Sea, 2006)

However, what might be interesting is after 1960 (See figure 4.3), when the Soviet government decided that the two rivers that fed the Aral Sea, the Amu Darya in the south and the Syr Darya in the northeast would be diverted to irrigate the desert, in order to attempt to grow rice, melons, cereals, and cotton.

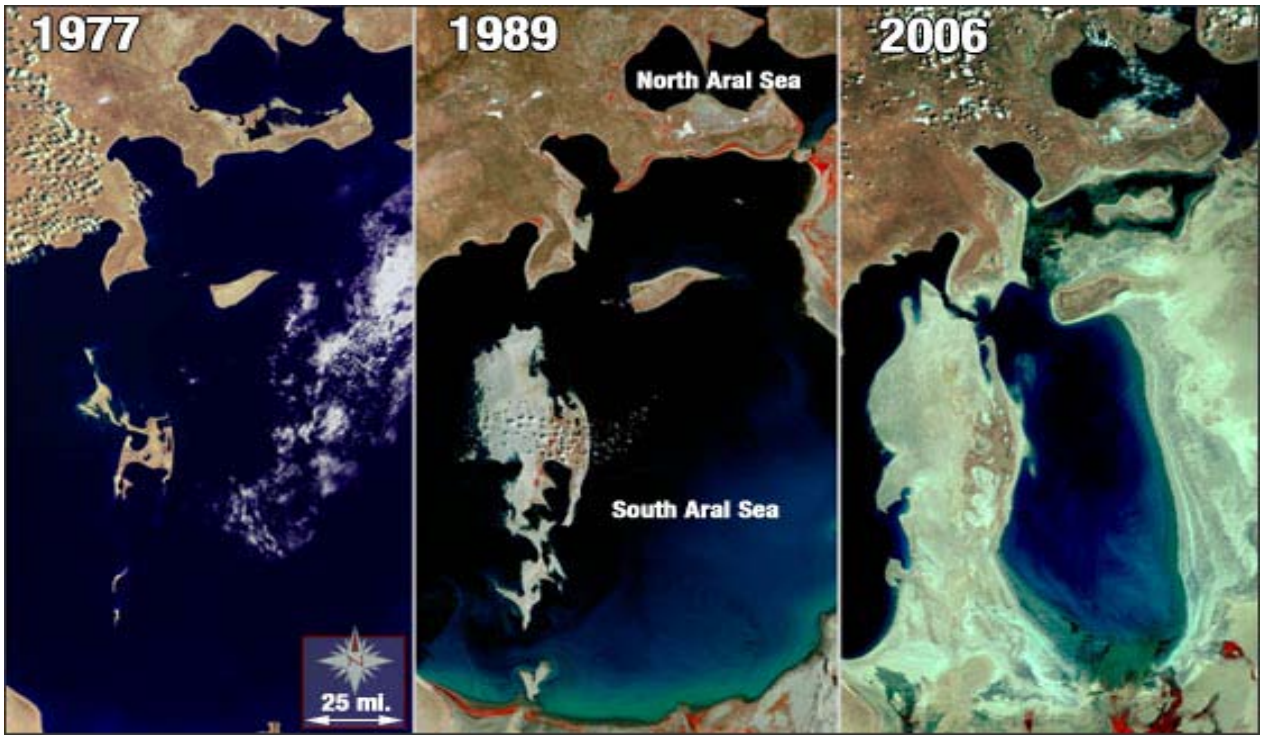

Figure 4.3 The change of Aral Sea during the past 30 years from 1997 to 2006. As we have mentioned before, the sea's surface area shrank by approximately 60% and its volume by 80%. For such a hot issue, I am interested to see if satellite altimetry could preciously monitor the change of water level height.

Figure 4.4 Orphaned ship in former Aral Sea, near Aral, Kazakhstan (Staecker, 2003).

Water loss is also caused by natural processes. Formerly one of the four largest lakes in the world with an area of 68,000 square kilometers, the Aral Sea has been steadily shrinking since the 1960s. From 1961 to 1970, the Aral's sea level fell at an average of 20 cm (7.9 in) a year; in the 1970s, the average rate nearly tripled to 50–60 centimeters (20–24 in) per year, and by the 1980s it continued to drop, now with a mean of 80–90 centimeters (31–35 in) each year. The rate of water usage for irrigation continued

to increase: the amount of water taken from the rivers doubled between 1960 and 2000, and cotton production nearly doubled in the same period, the sea's surface area shrank by approximately 60% and its volume by 80%.

The ecosystem of the Aral Sea and the river deltas feeding into it has been nearly destroyed, not least because of the much higher salinity. The receding sea has left huge plains covered with salt and toxic chemicals – the results of weapons testing, industrial projects, pesticides and fertilizer runoff – which are picked up and carried away by the wind as toxic dust and spread to the surrounding area. The land around the Aral Sea is heavily polluted and the people living in the area are suffering from a lack of fresh water and health problems, including high rates of certain forms of cancer and lung diseases. Respiratory illnesses including tuberculosis (most of which is drug resistant) and cancer, digestive disorders, and infectious diseases are common ailments in the region. Liver, kidney and eye problems can also be attributed to the toxic dust storms. Health concerns associated with the region are a cause for an unusually high fatality rate amongst vulnerable parts of the population. Crops in the region are destroyed by salt being deposited onto the land. Vast salt plains exposed by the shrinking Aral have produced dust storms, making regional winters colder and summers hotter. The Aral Sea fishing industry, which in its heyday had employed some 40000 and reportedly produced one sixth of the Soviet Union's entire fish catch has been devastated (www.en.wikipedia.org/wiki/Aral_Sea).

4.2.3 Amazon basin

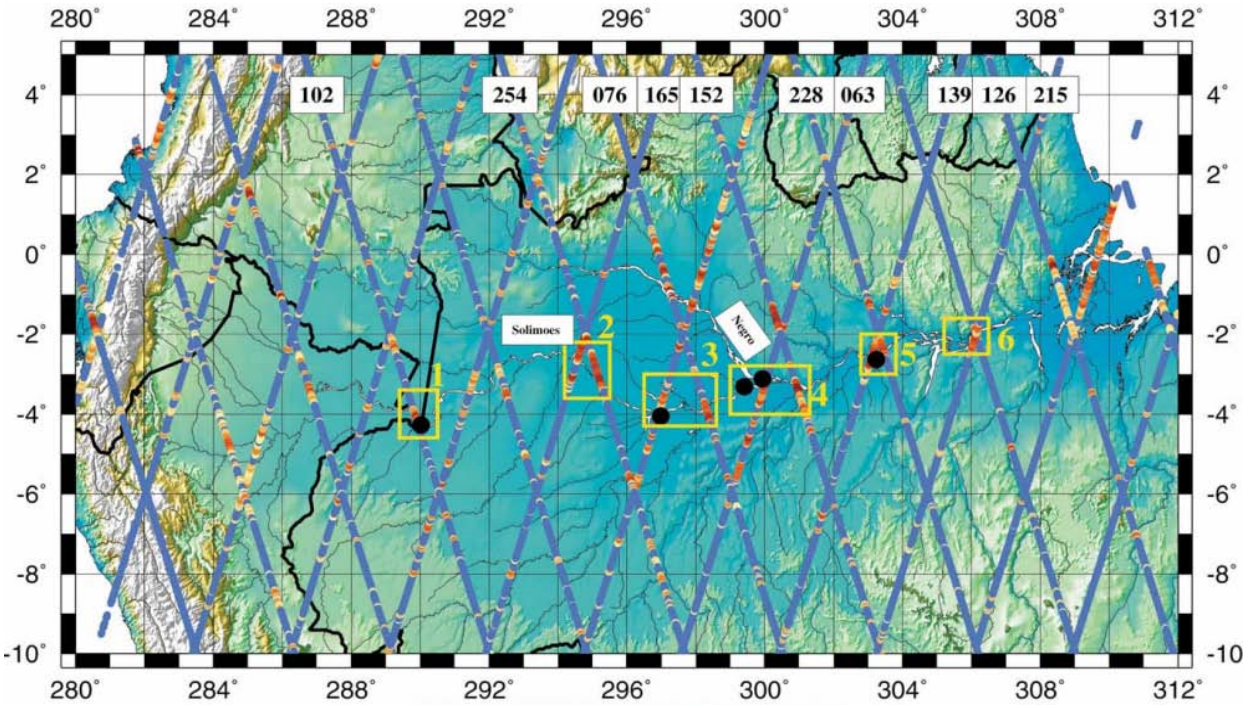

Figure 4.5 The Topographic map of the Amazon basin on which are superimposed the Topex/Poseidon satellite tracks (identified by their number). Yellow boxes correspond to areas selected in the present analysis. Black dots show the position of the in-situ water gauges: stations of Tabatinga (box1), Itapeua (box3), Manacapuru and Manaus (west and east respectively in box4) and Parintins (box5) (Oliveira Campos, 2001).

Amazon River is one of the most typical inland water bodies of previous research. And in my study, I would like to generate the water level change from 1992 to 2002, and meanwhile, show the annual behavior and season behavior of such a big river. By comparing with the in-situ gauge data, accuracy of T/P will be evaluated as well.

4.3 Methodology

To begin with, I would like to take the case in Amazon River for example (Figure 4.6).

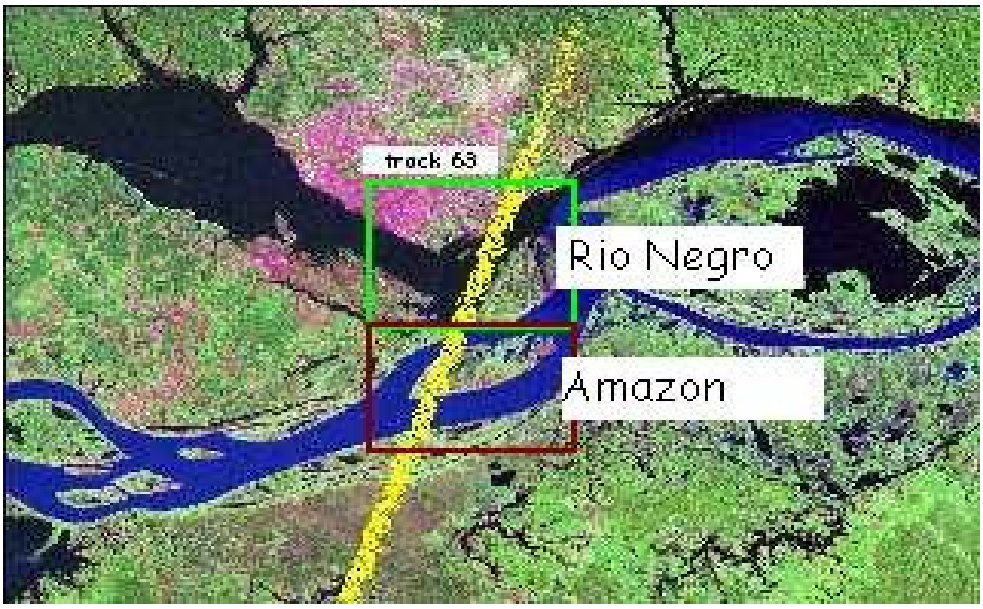

Figure 4.6 The Amazon River together with T/P track No 63. Since this section of river is only 5.7 km in width. So the number of 10 Hz footprint will be no more than 10, considering that inside the water body there are 2 island, corresponding waveforms (probably a half of them)are supposed to be noisy, which should be detected and removed automatically before waveforms retracking, aims at improving the data quality and better accuracy.

In this process, we are dealing with large quantities of MGDR data and waveforms from SDR data, in the above figure 4.6, since there are 10 footprints inside Amazon River per Cycle, and from 1992 to 2002 there are altogether 364 valid cycles, thus we have 3640 waveforms (10 Hz)of all. In principle, we are supposed to deal with all of them one after another, actually in practical it is not necessary to do so, due to the fact that some waveforms might be too noisy to analyze, and figure 4.7 shows randomly a group of them.

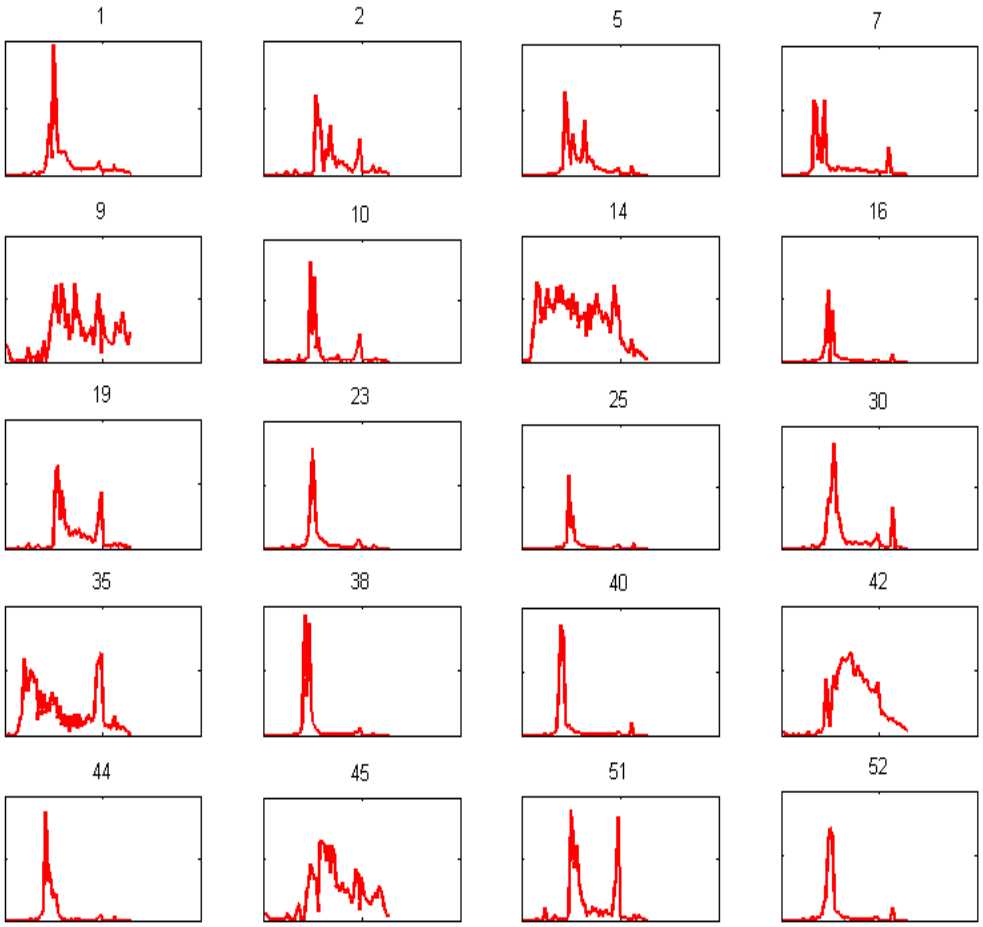

Figure 4.7 A group of waveforms from Amazon River, the title of each subplot means the random chosen cycle number.

From the above figure, in cycles 1, 10, 23, 25, 38, 40, 44, 52, we find waveforms with single sharp peak, in our study, they are actually pretty good waveforms as expected, since the leading edge is clear and easy to find. While looking at the other waveforms, such as cycle 9, 14, 35 and 45, which are very noisy due to several reasons, in practice, it is difficult or even not possible to find where the leading edge is, and we cannot derive any useful information from such waveforms.

4.3.1 Noisy Waveform Detection

As we have discussed in Chapter 2, when satellite altimetry is applied in non-ocean surface, waveforms become noisy due to complicated topography. Therefore, in my study, such so call “Noisy waveforms” are supposed to be filtered out at the very beginning.

Here we have 2 waveforms as follows in figure 4.8:

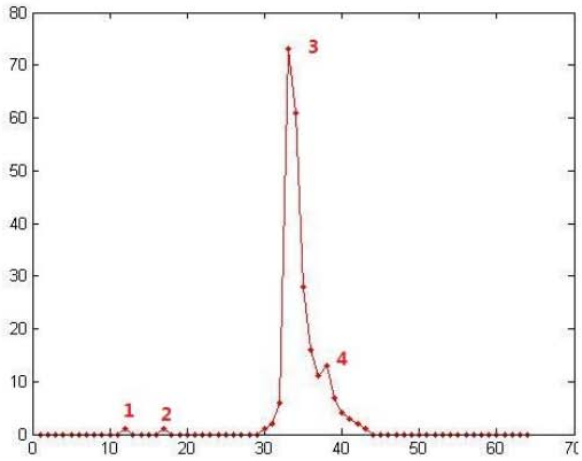

Figure 4.8 (a)

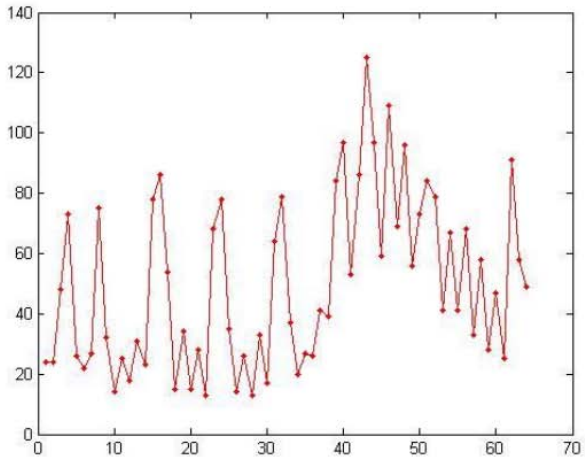

Figure 4.8 (b)

To begin with, we should find out how many waveforms exist in a given waveform. Based on the number of waveform we can further check if the waveform is noisy or not.

In principle, if there is a peak, it should satisfy:

$$p_{n-1} < p_n > p_{n+1} \tag{4.1}$$

We find 4 peaks exist in **Figure 4.8 (a)**. However, according to our experience, only peak $\mathrm{No.3}$ can be regarded to be a real peak, and for the others, which are merely tiny noise of signal.

Therefore, a threshold K must be defined to check if a peak can be regarded to be a peak or not.

$$\left|p_n - p_{n-1}\right| + \left|p_n - p_{n+1}\right| > K \tag{4.2}$$

Function (4.2) should be satisfied if there is a peak, finally there are N peaks all together for a given waveform. Here it should be noted that, the value K cannot be too big, since real peaks might be ignored. It cannot be too small either; otherwise, the tiny signal noise might be regarded as a real peak.

Then, another threshold should be defined as well to judge a noisy waveform: the number of peaks N_0.

$$N > N_0 \tag{4.3}$$

Once both function (4.2) and (4.3) are satisfied, we can safely say that this waveform is a noisy waveform according to our expectation.

To define what a noisy waveform is, (for the purpose of detect and remove the noisy waveforms automatically), the key point is the proper choice of values K and N_0, here it should be mentioned that the choice might be various depending on different water properties. In this study, we tried different

groups of values K and N_0, here I take again the Amazon River for an example, and list 3 groups from all the tests we have tried.

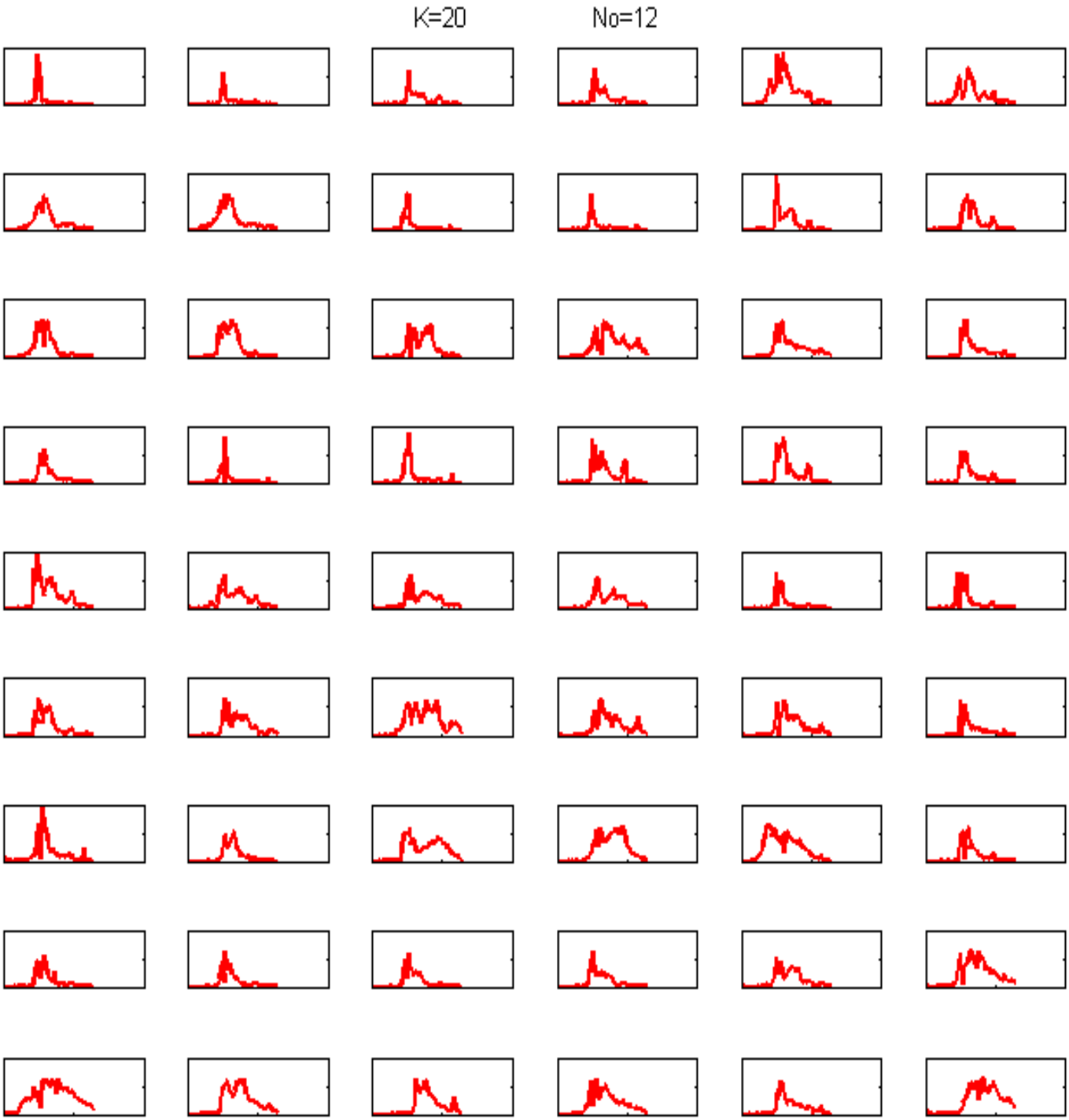

Figure 4.9 (a) $K = 20, \quad N_0 = 12$ In this group we set the threshold number of peaks to be 12, actually from the result it shows that 12 is a pretty big value, since still a lot of noisy waveforms exist after filtering, then we will try to use a smaller threshold value.

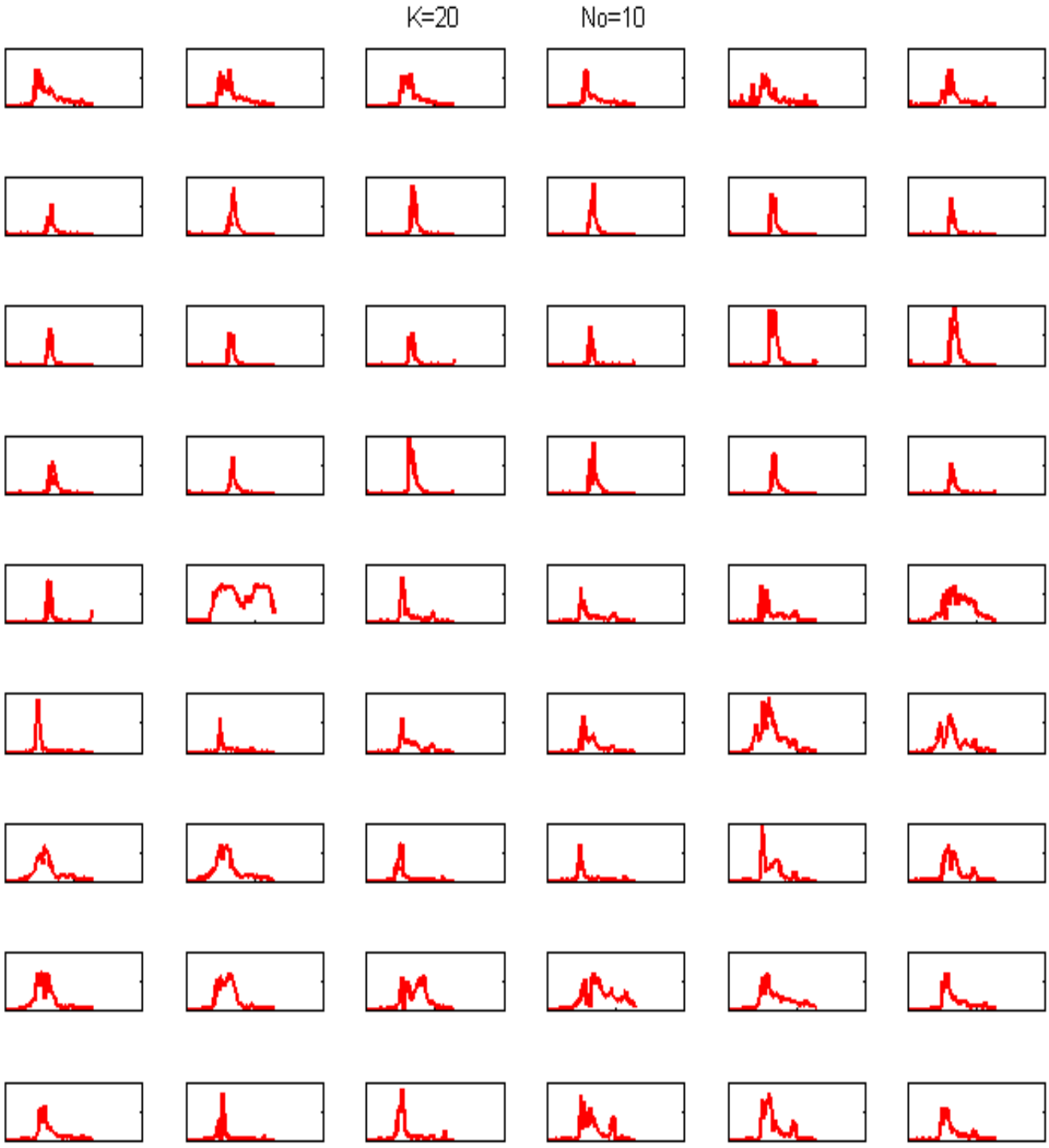

Figure 4.9 (b) $K = 20, \quad N_0 = 10$, based on the case in figure (a), here we reduced the threshold value of peak numbers to be 10, from the result we find more noisy waveforms are filtered out, but still some of them exist, so we have to try even smaller threshold values again.

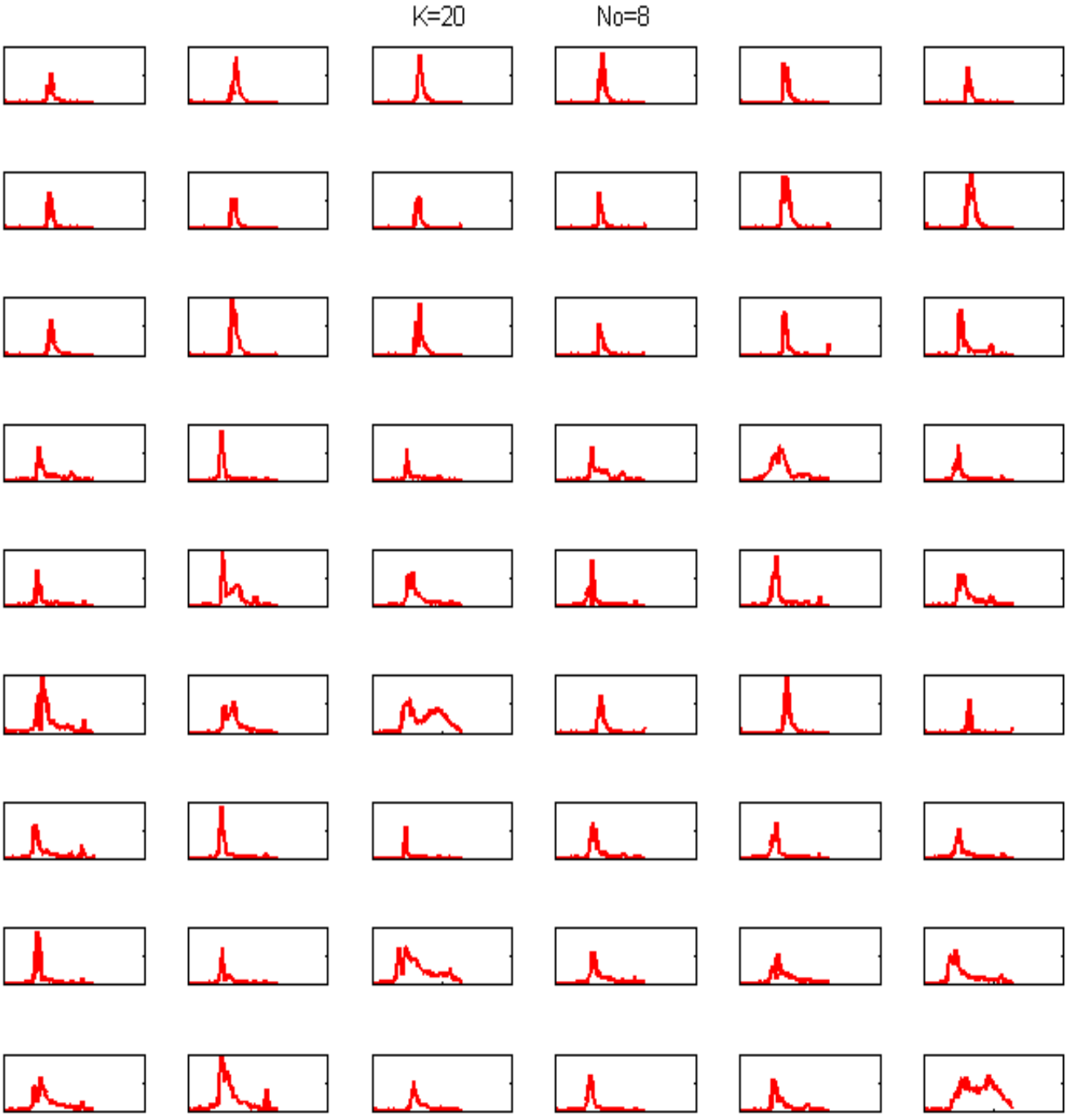

Figure 4.9 (c) $K = 20, \quad N_0 = 8$, this time we reduced again the threshold value of peak numbers to be 8, and finally no noisy waveforms exist anymore.

Now, I summarize the above selected 3 groups of data into the following table.

Table 4.1 Proper Choice of Threshold Values to detect Noisy Waveforms

Result / Choice	Waveform Removed (%)	Check
$K = 20, \quad N_0 = 12$	15.2	Majority waveforms are noisy
$K = 20, \quad N_0 = 10$	24.1	Half of all waveforms are noisy
$K = 20, \quad N_0 = 8$	37.6	No Noisy waveforms exist

In this study, we tried more than 10 groups of threshold values to remove noisy waveforms, and according to the result, here I choose $K = 20, \quad N_0 = 8$ to detect and remove noisy waveforms. Again, here are several important facts to be made clear:

- The choice of threshold values is not unequal for a given water body. Normally, the smaller value you choose, more waveforms will be removed, and good waveforms might be removed as well. Thus threshold values should be selected carefully.
- For different water bodies, the threshold values are different as well, depending on the properties of individual topography.

4.3.2 Optimal Retracking

After removing all the above so called "Noisy waveform", the next step is waveform retracking. Since we have different retracking algorithms: OCOG, Threshold and Beta 5, in principle, we can do all the waveform retracking with single method, but still, in this study, we tried to make a sufficient combination of different algorithms, considering that each algorithm has its own advantages and disadvantages.

To combine different retracking methods together, our basic idea is: normally, Beta 5 retracker is regarded to be the best fit of a given waveform, so the retracked result is supposed to be more reliable than the other methods, thus, in this study, we gave priority to Beta 5 algorithms. Meanwhile, the weakness of this method is: this algorithm could only be applied to certain waveforms with shape close to "Brown Model", for the other waveforms, we should consider OCOG and Threshold.

In principle, threshold 50% retracker is proved to be particular suitable for waveforms with sharp peaks and clear leading edge (Guo J.Y., 2010), thus, we give second priority to threshold retracker.

And finally, OCOG algorithm is less preferred due to low accuracy; however, OCOG method is still used to provide initial values for other algorithms.

Figure 4.10 shows the results of single retracking and optimal retracking. And from figure 4.10, it is not difficult to find that: lake level height generated by optimal retracking is much more close to in-situ gauge data, compared with single retracking results.

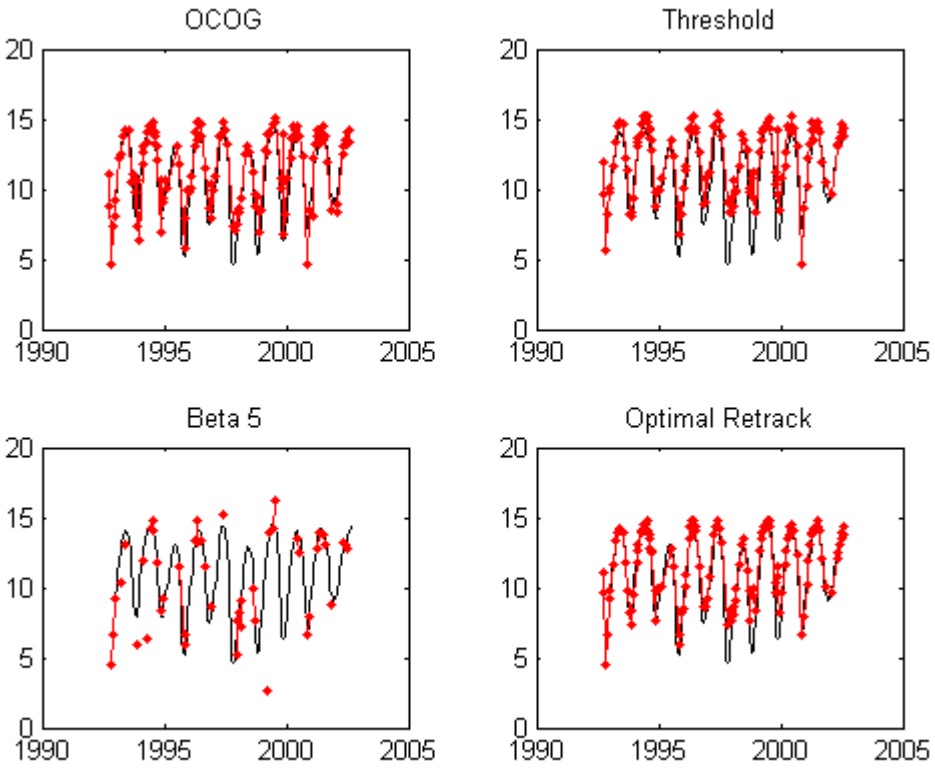

Figure 4.10 Time series of lake level height derived from single retracking method and optimal combination of different algorithms, black line means in-situ gauge data and red dots stand for T/P results.

4.4 Results

In this section, I would like to present the water level height of selected water body derived from Satellite Altimetry (Topex/Poseidon), furthermore, water level height after retracking will be derived as well to compare with the non-retracking data, for the purpose of evaluating the accuracy of satellite altimetry. Finally, by comparing with the already existing in-situ data, further discussion will be made to verify the potential of satellite altimetry for inland use.

In section 4.2 we have already given preference to three different water bodies, Huron lake, Aral Sea and Amazon River, which are all inland water bodies in common, but still different due to the facts that: Huron lake is a vast water body with broad surface similar to ocean, since satellite altimetry was initially designed for vast ocean use, so in my study I choose Huron lake just for the purpose of verifying the optimal performance of satellite altimetry (Topex/Poseidon). While Aral Sea is a relatively smaller inland lakes, with sharply change of water level and complicated environment. Finally Amazon River is a vast water system with many tributaries but narrow in width, therefore, environment is extremely complex; actually it is my interest to investigate its capability of monitoring such inland water bodies.

4.4.1 Huron Lake

In my study, Topex/Poseidon 10Hz data from cycle 1 to cycle 364 (1992-2002) is used. From Figure 4.10 shows that all together there are 3 tracks which go across Huron Lake, they are No 240, No 117 and No 152, here I only use the data of track No 117, considering this track goes exactly above a nearby in-situ gauge station (Harbor Beach, MI 9075014, red point in figure 4.11), which provides lots of convenient for evaluation of Topex measurement.

All added together, we used 110 footprints of 10Hz along-track, from cycle 1 until cycle 364; finally, there are 40040 waveforms to be analyzed, which is huge quantity of data.

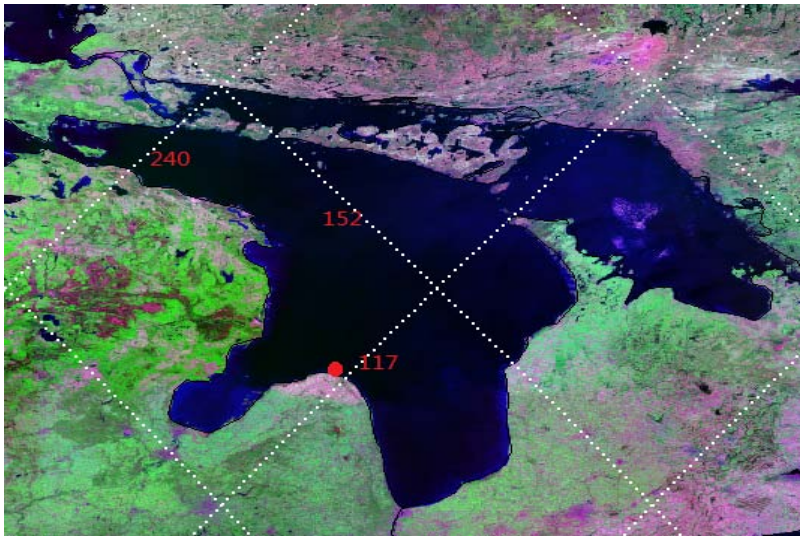

Figure 4.11 Huron Lake with 3 T/P tracks inside, No 240, No 117 and No 152, red dot represents in-situ gauge station named Harbor Beach.

Since topography in Huron Lake is similar with Ocean surface, we can predict that data quality is supposed to be pretty good. And actually our prediction has been verified by **Figure 4.12**.

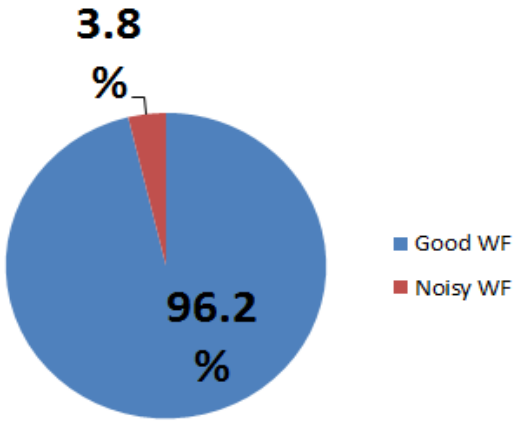

Figure 4.12 Data quality in Huron Lake, 96.2% are good waveforms while the rest 3.8% are regarded to be noisy.

Finally we generated time series of Lake Level Height of Huron Lake (See Figure 4.13).

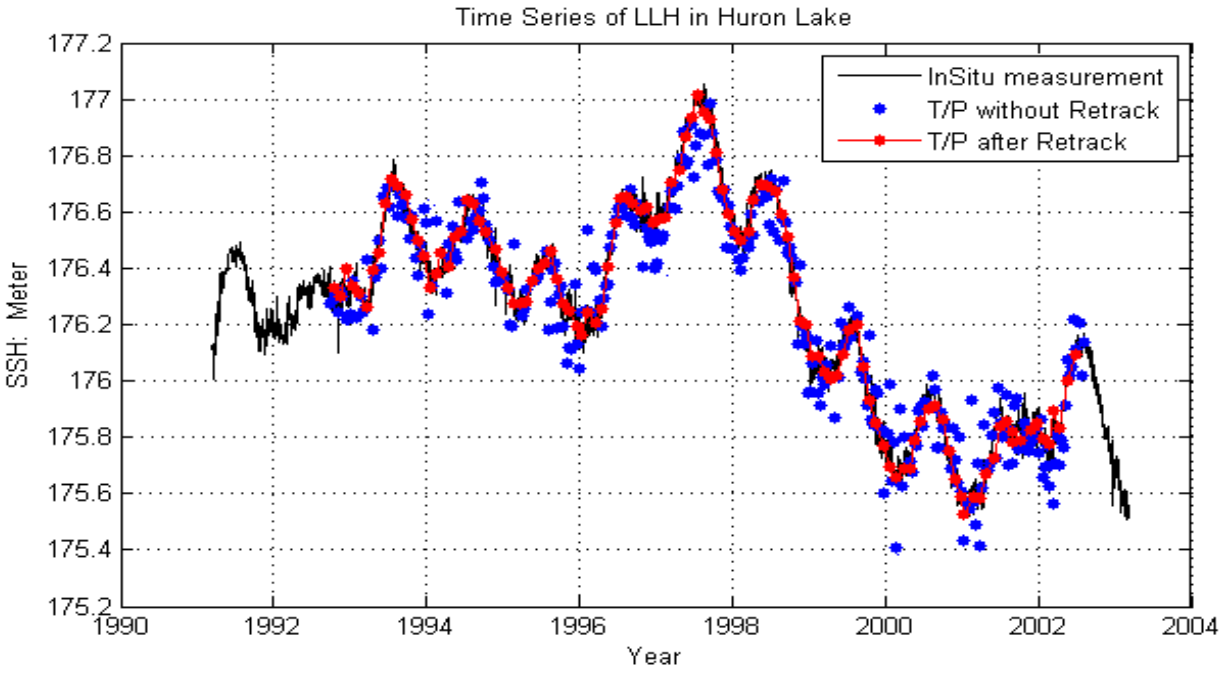

Figure 4.13 Time series of Lake Level Height in Huron Lake from 1992 to 2002. Blue dots represent T/P SSH before retracking. Red line represents T/P SSH after retracking, while Black line represents In Situ station measurement.

For better understanding of the T/P results, we subtract both LLH before retracking and after retracking by in-situ gauge data (as showed in figure 4.14), calculate their corresponding RMS (Root Mean Square) and Mean, then we can see clearly how much difference T/P values vary from In-situ gauge data (as reference).

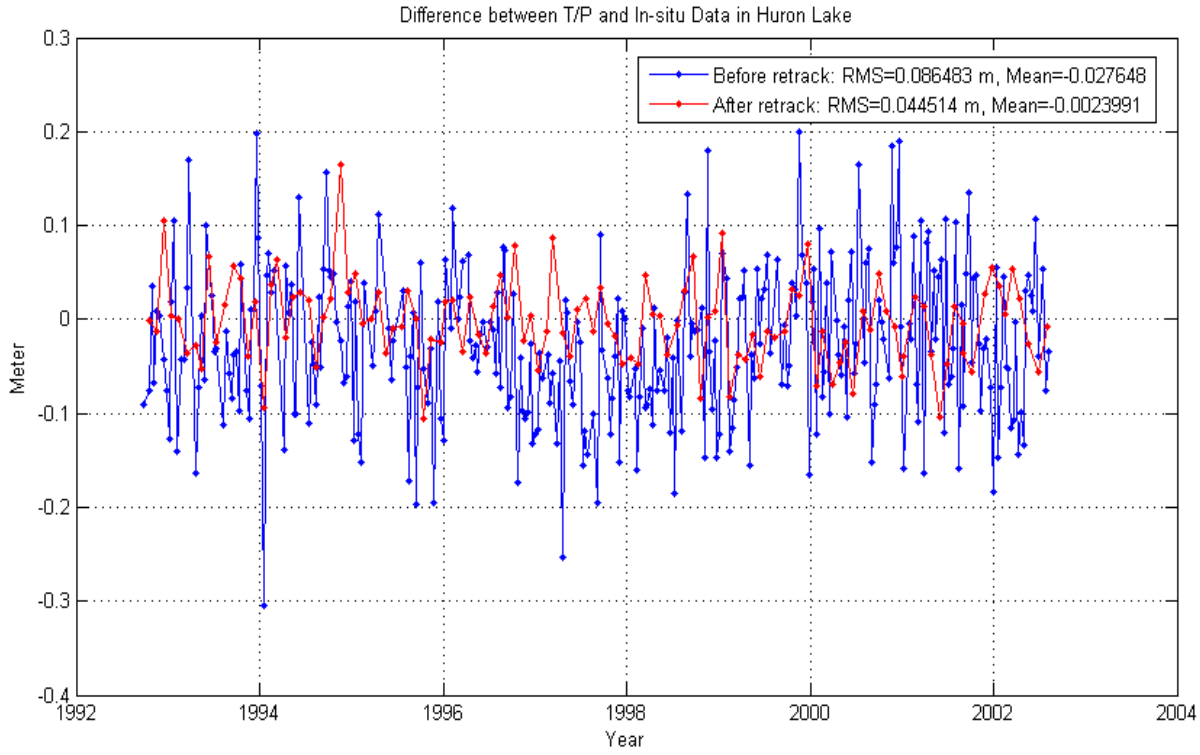

Figure 4.14 The difference between the T/P LLH and the in-situ gauge data. Blue line represents the difference between T/P data and In Situ data before retracking, RMS=8.6cm, the mean value is -27.6 mm. Red line represents the difference between T/P data and In Situ data after retracking, RMS=4.5cm, the mean value is only -2.4 mm.

Generally speaking, T/P shows great performance among water bodies with broad surface, in Huron Lake accuracy of T/P after retracking could reach up to 4.5 cm's level, which is consistent with the official announcement that satellite altimetry was designed to measure vast oceans with centimeter's accuracy.

4.4.2 Aral Sea

For vast ocean T/P performs well, now let us investigate how it works in a relatively small water body, Aral Sea.

Similarly with Huron Lake, we still use Topex/Poseidon 10Hz data from cycle 1 to cycle 364 (1992-2002) for Aral Sea. From Figure 4.14 we can see there are 2 tracks which go across Aral Sea, they are No 107 and No 142, here I gave preference to No 107, since it is less affected by the island inside Aral Sea, and track No 107 provides more data than No 142 as well.

This time, we used only 50 footprints of 10Hz along-track, from cycle 1 until cycle 364; finally, there are 18200 waveforms to be analyzed, which is still huge quantity of data.

Figure 4.15 Aral Sea with T/P track inside.

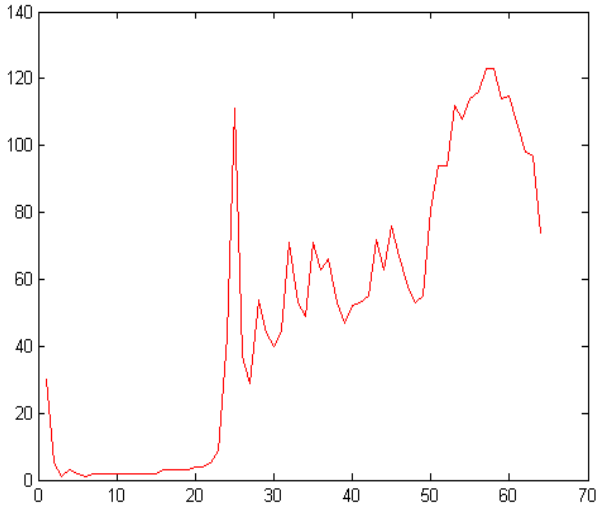

Figure 4.16 Typical waveform in Aral Sea

Figure 4.16 shows the typical waveform in Aral, very interesting we find that the typical waveforms of Aral Sea have 2 peaks, with one of them to be the real leading edge around the bin 25, and the other located at trailing edge. This strange phenomenon is supposed to be caused by the particular topography of Aral Sea. Look at Figure 4.15, since the main body of Aral Sea has been divided into two parts due to the falling of water level, therefore, signal from satellite radar firstly will touch the east part of water body and form a peak in the real leading edge, while the later peak might be reflected from the west part of water body.

Here, it should be mentioned that to deal with such strange waveforms, especially during the waveform retracking process, OCOG method should be avoid due to the irrational distribution of power, in practice, threshold 50% method is preferred, anyway, the for majority of waveforms in Aral Sea, the leading edge is clear.

Again, data quality of Aral Sea should be tested at the very beginning in figure 4.17.

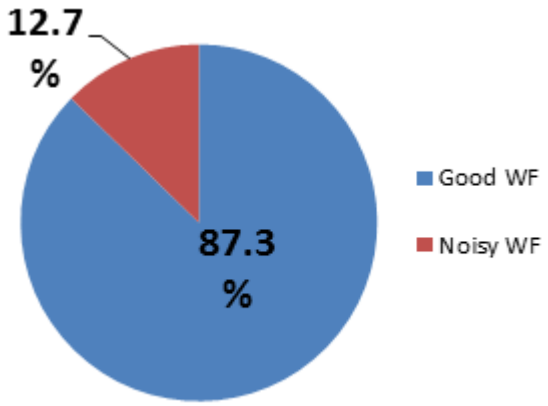

Figure 4.17 Data quality of Aral Sea, which shows that in Aral Sea 87.3% of all waveforms are seemed to be “Good”. Here I selected random a group of the “Bad waveforms”.

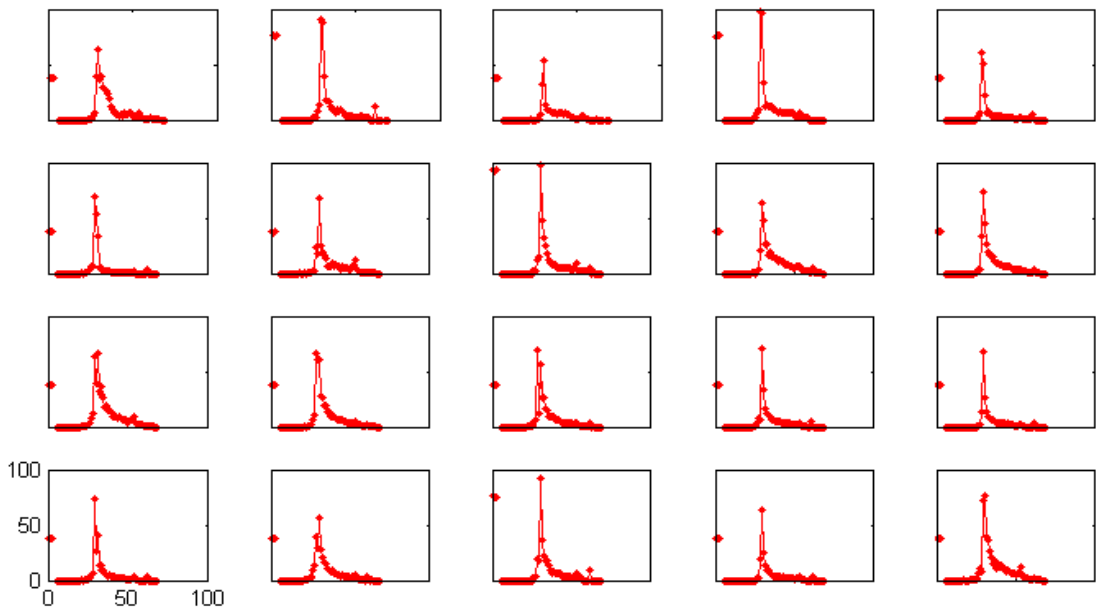

Figure 4.18 A group of so call "Bad" waveforms; actually, it is hard to say they are noisy, in contract, they are pretty ideal in shape. The reason why I filter them out is because of their weak power. Since satellite radar altimeters is originally designed for water measurement, thus the power reflected from water surface should be bigger than 100 or so, otherwise, the waveform is not reliable, despite whatever shape of it.

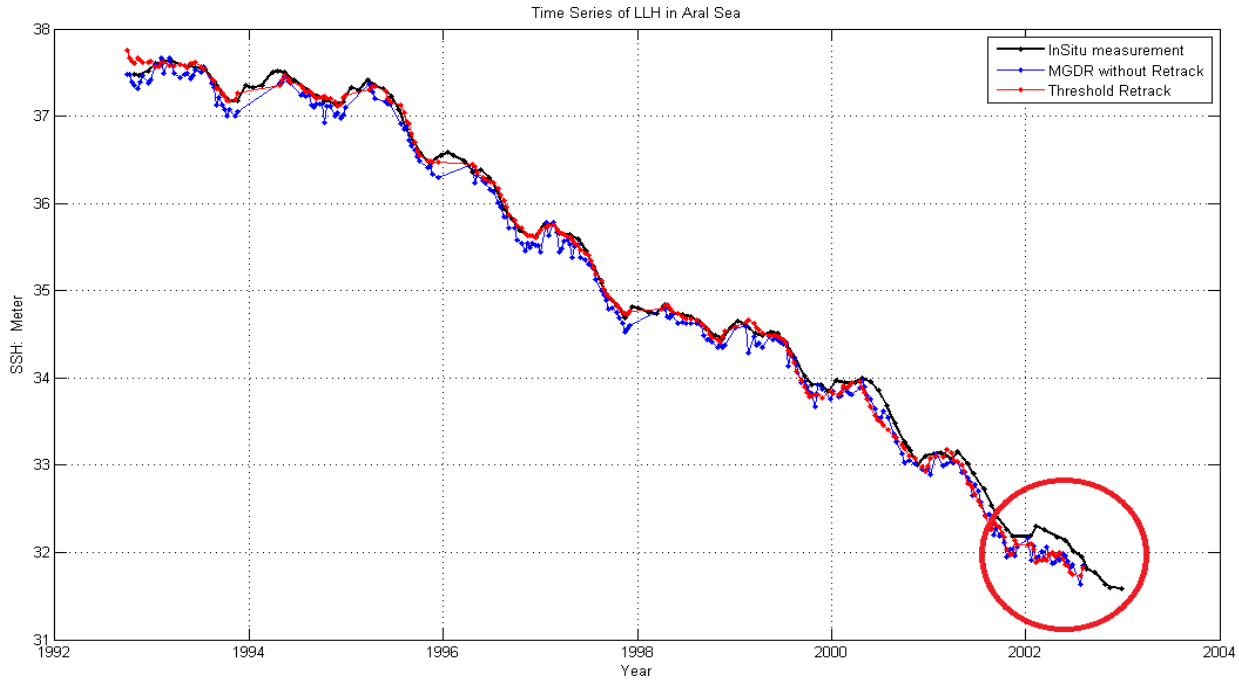

Figure 4.19 shows time series of Lake Level Height in Aral Sea from 1992 to 2003. Blue dots represent T/P SSH before retracking. Red line represents T/P SSH after retracking, while Black line represents In Situ station measurement. And in the red cycle we find that there is relatively larger deviation between T/P result and in-situ result, which might be explained by: after the year 2002, water in Aral Sea is in such a low level that T/P could not measure as accurate as before.

Again, for better analysis of the T/P results, we subtract both LLH before retracking and after retracking by in-situ gauge data, derive corresponding RMS and mean value (figure 4.20), and see how much difference T/P values vary from In-situ gauge data (as reference).

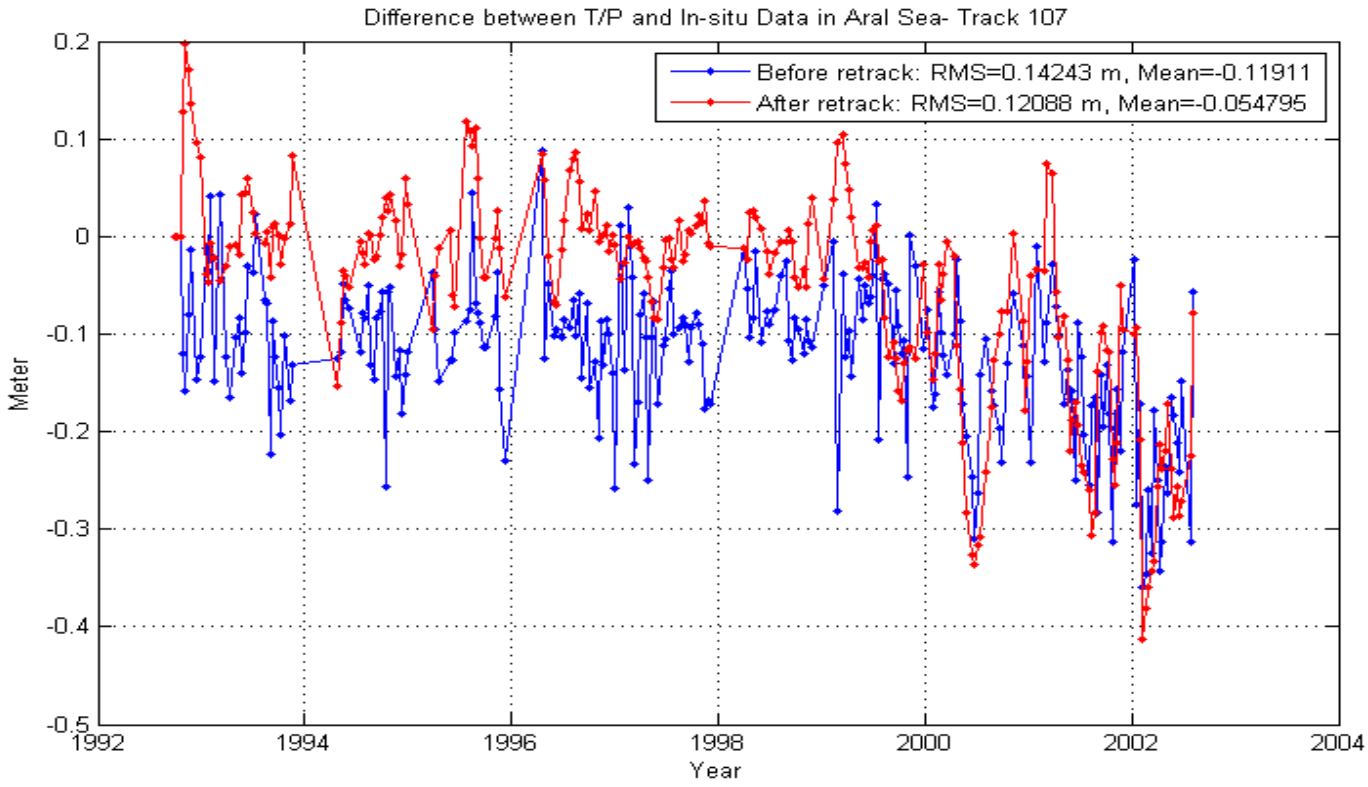

Figure 4.20 The difference between the T/P LLH and the in-situ gauge data. Blue line represents the difference between T/P data and In Situ data before retracking, RMS=14.2cm, the mean difference is -119 mm. Red line represents the difference between T/P data and In Situ data after retracking, RMS=12.1cm, and the mean difference is -55 mm, which is much smaller than that of before retracking, so bias reduces.

In general, 12.1 cm is still good accuracy for most hydrologic application. However, in Figure 4.20 what attracts me most is: Before the year 2000, T/P measurement seems to be more accurate than that after the year 2000, in specific, during the period of 1993 to 1999, water level could be determined very precisely by T/P within 5 cm, after that, accuracy decreased up to 20 cm or even worse with respect to time.

One possible explanation might be found in Figure 4.19, which we can clearly observe that water level height of Aral Sea keeps decreasing with time (1992 – 2001 in my study). Therefore, we can imagine that the accuracy of satellite altimetry is closely affected by the depth of water.

4.4.3 Amazon River

For large water bodies like Huron Lake and Aral Sea, we have verified that T/P performs well; then we would like to investigate some more challenging area, Amazon River, see how satellite altimetry works in such a narrow environment.

In Amazon River, we still use Topex/Poseidon 10Hz data from cycle 1 to cycle 364 (1992-2002). From Figure 4.20 we can see there is only one track that goes across Amazon River, it is track No 63, since the river is only 6 km in width, thus the number of 10Hz footprint within such as river will is limited (10 for maximum). Moreover, we find two islands inside the river, that means the number of footprints inside real water body will be even less, and of course corresponding waveforms are supposed to be affect by the island, which brings more errors into satellite radar measurement.

This time, we used only 10 footprints of 10Hz along-track, from cycle 1 until cycle 364; finally, there are 3640 waveforms to be analyzed.

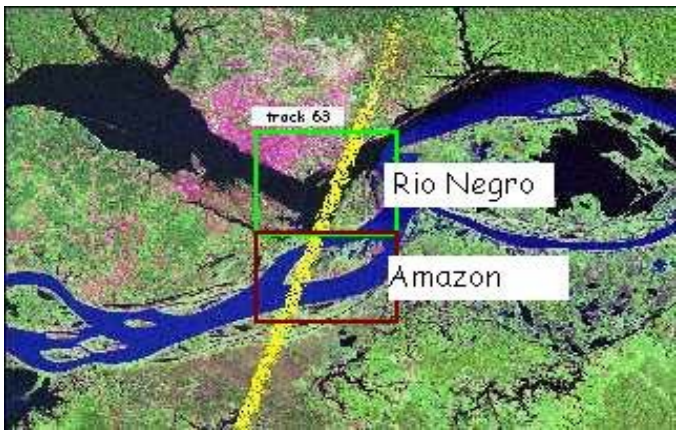

Figure 4.21 Amazon River with T/P track No 63.

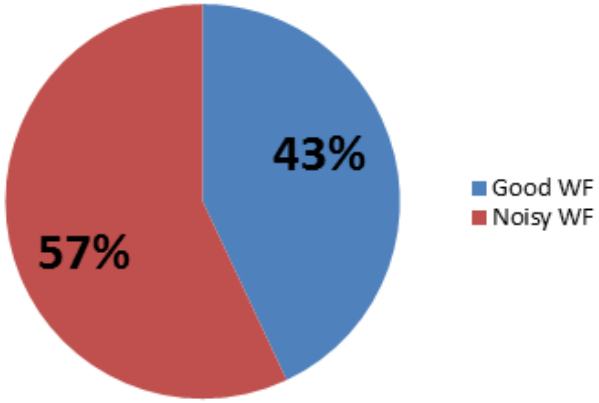

Figure 4.22 Data quality of Amazon River

Figure 4.22 shows data quality of Amazon River, majority of waveforms (57%) is regarded as "Noisy" waveforms, which is bad data quality as expected. Here, I will list several random cycles of waveforms.

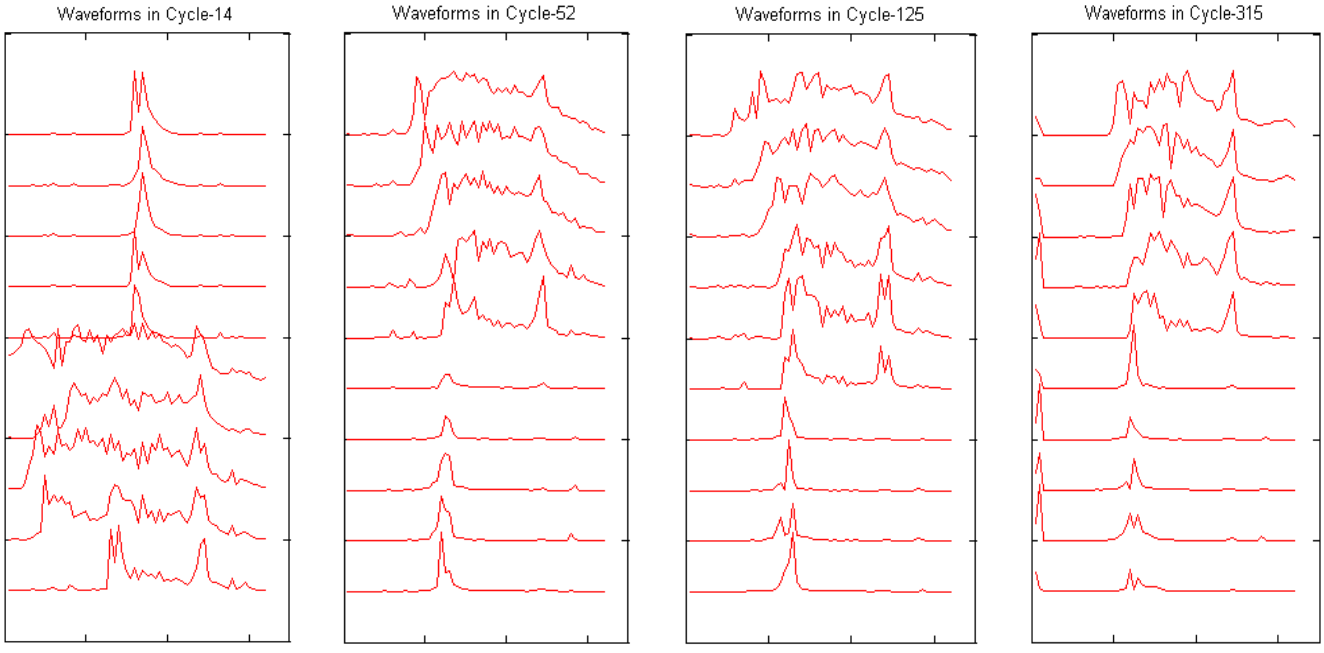

Figure 4.23 (a) **(b)** **(c)** **(d)**

We believe that Figure 4.23 already provides reasonable explanation why data quality in Amazon River is so bad, since the water surface of a river is relatively narrow comparing with huge lakes, thus, not all waveforms are reflected from water surface, some of them from valid land actually.

To deal with such situation, I just simply delete waveforms that come back from valid land or forest, it is quite reasonable to do this, anyway, we are dealing with water.

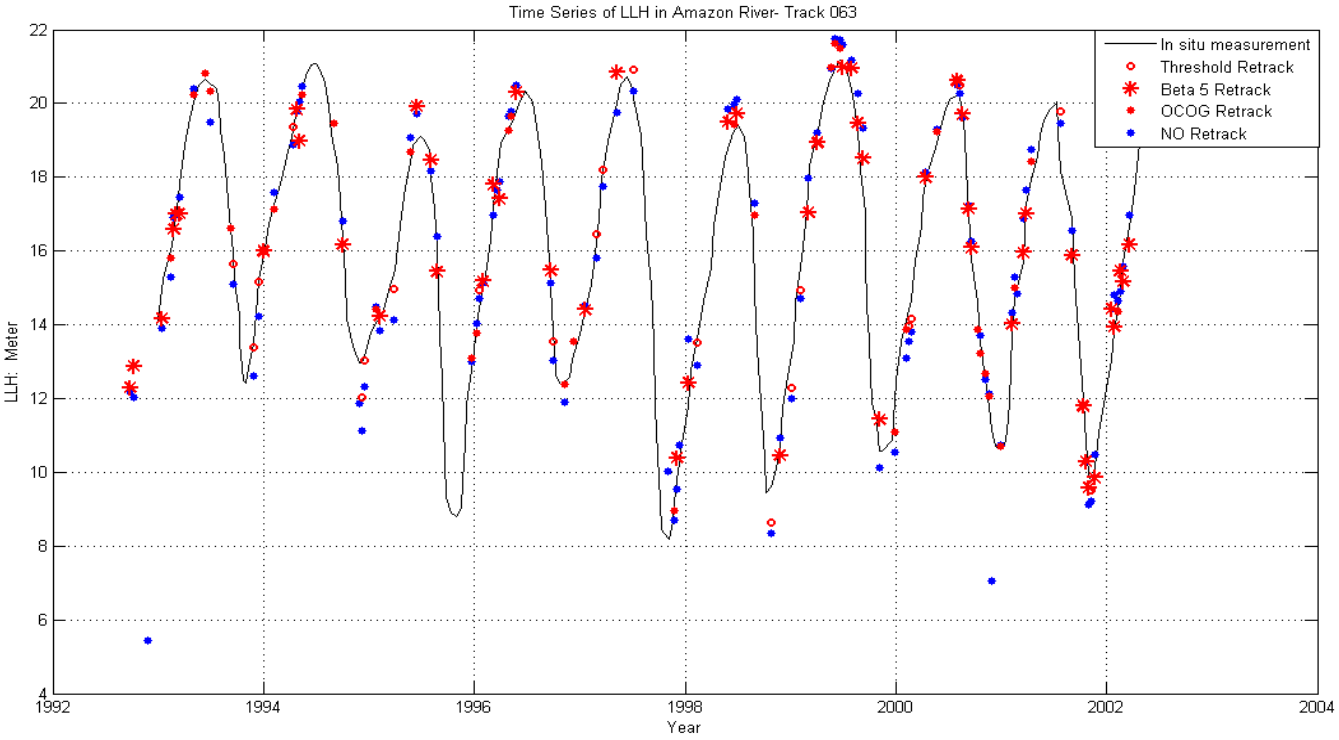

Figure 4.24 Time series of Water Level Height in Amazon River from 1992 to 2002. Blue dots represent T/P SSH before retracking. Red dots represent T/P SSH after retracking, while Black line represents In Situ station measurement.

In general, T/P data in Figure 4.24 seems to be sparsely distributed, especially when it comes to dry seasons with low water level in winter, T/P fails to measure the water level height preciously, even worse, for some period of time (Winter of 1995 and 1997), and there is no useful measurement at all.

Again, for better analysis of the T/P results, we subtract T/P measurements by in-situ gauge data, then derive RMS and the mean difference (Figure 4.25), and see how much difference T/P values vary from In-situ gauge data (as reference).

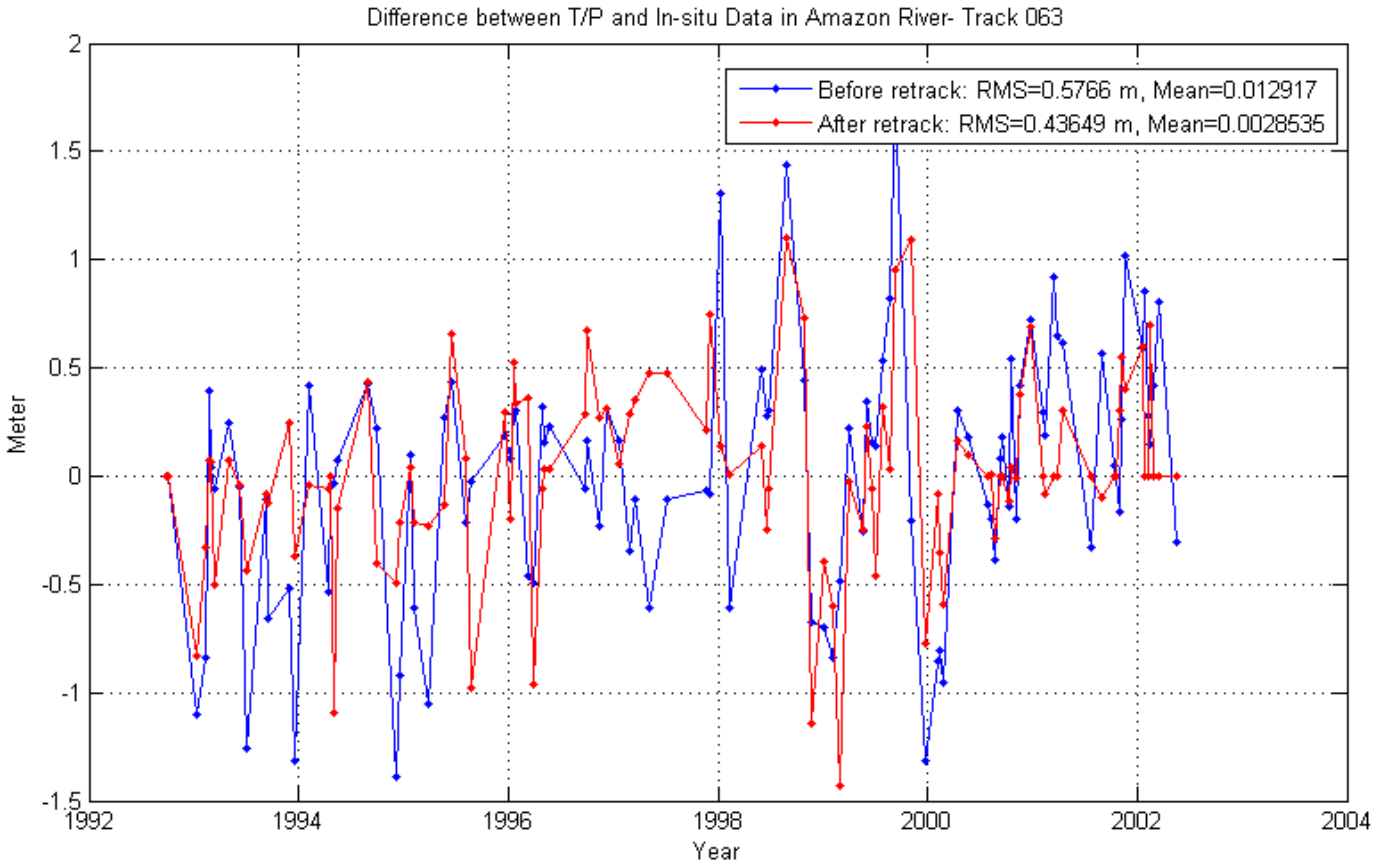

Figure 4.25 The difference between the T/P LLH and the in-situ gauge data. Blue line represents the difference between T/P data and In Situ data before retracking, RMS=57.9cm, the mean value is 13 mm. Red line represents the difference between T/P data and In Situ data after retracking, RMS=43.8cm and the mean value of difference reduces to only 3 mm, again the mean value of residuals is much smaller than that of before retracking, so bias reduces again.

In Amazon River, accuracy of T/P is roughly half a meter, which are definitely not ideal results. Therefore, for the purpose of precisely monitoring water level change of inland rivers, satellite altimetry is not preferred comparing with traditional solutions.

4.5 Summary

In this section, I put together all the results (data quality in figure 4.26 and lake level height information in figure 4.27) from selected water bodies.

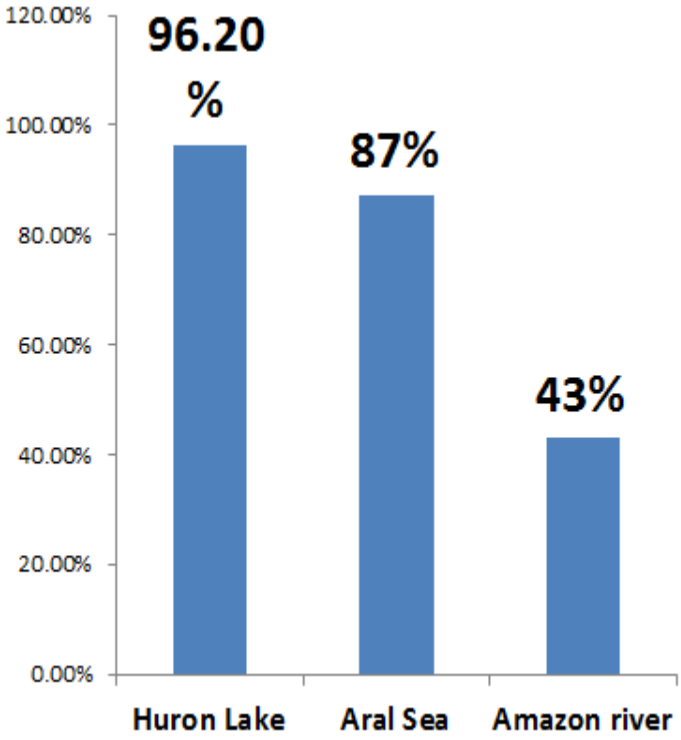

Figure 4.26 Data quality

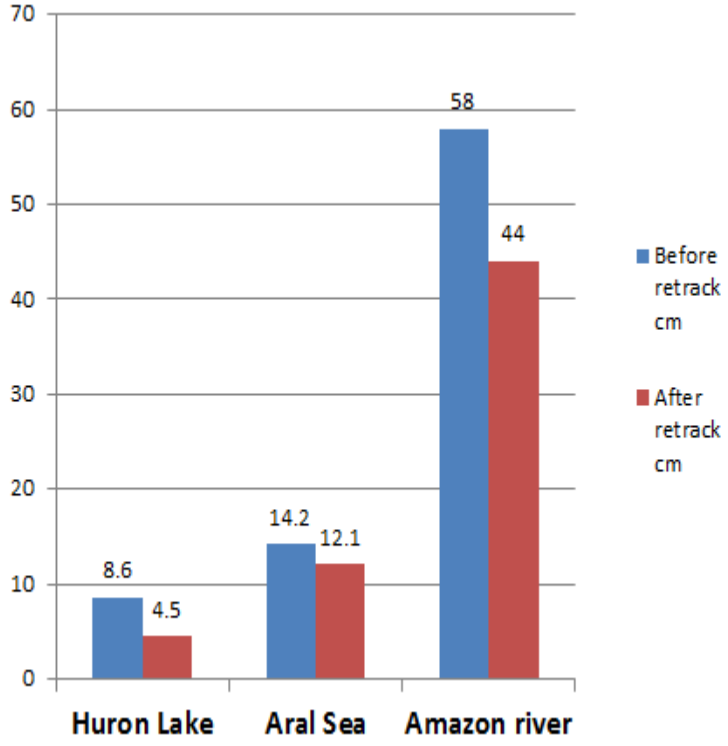

Figure 4.27 Accuracy of T/P

- Figure 4.26 shows the data quality of T/P for different water bodies. The larger water body, the better data quality can be achieved. Since it is less affected by the topography and environment.
- Figure 4.27 shows the accuracy of T/P measurement for each of the selected water body. Again, the larger water surface, the higher accuracy could be achieved. Meanwhile, for all selected water bodies, waveform retracking is verified to be an effective solution to overcome the effects of errors and improve the accuracy of satellite altimetry.

Chapter 5

CONCLUSIONS

Satellite Altimetry, which was initially designed for the study of global sea surface height with centimeters accuracy, has been demonstrated to be usable to non-ocean surface as well. In this study, three different targets have been examined: Huron Lake, Aral Sea and Amazon River. In addition, we retrieved the individual 10-Hz retracked data, assessed the performance of 10-Hz retracked data in measuring the continental water level.

In chapter 4, to access the accuracy the satellite altimetry (Topex/Poseidon), we firstly choose a large lake (Huron Lake), and in which there are available in-situ gauge stations for comparing both the retracked Topex data and non-retracked data with high-accurate in-situ gauge data. The comparison are conducted by computing the difference between the Topex data and the in-situ gauge data, then calculate the Root Mean Square and mean values for each of them. The results show that the accuracy of T/P data increases from 8.6 cm to 4.5 cm after retracking, and bias reduced as well, which indicates the accuracy improvements using the retracked data.

Following the assessment of the accuracy of the individual 10-Hz retracked data, we provided the 10-Hz measurement of smaller bodies of water: Aral Sea. Similarly, time series of water level height is derived from the average value of each 10-Hz measurement, but in this case, since the water surface is relatively smaller and the waveforms are more affected by the surrounding environment, to improve the accuracy of each retracked waveform, we designed a waveform filter aims at detecting and removing waveforms with lower quality, finally, more than 10% of all waveforms are removed, from the result, which shows that in Aral Sea accuracy of Topex data decreased to 14.2 cm before retracking and 12.1 cm after retracking. Despite that we got lower accuracy than Huron Lake, we found that before the year 2000 Topex still provide competitive (5 cm) accuracy when the water level is pretty high, only after the year 2000, when water level height became lower and lower, accuracy of Topex decreased, which indicates that Topex is particular suitable to be applied for large scale of water bodies.

Finally, we come to Amazon River, for the application of Topex/Poseidon; this is an extreme situation due to several reasons: Narrow water body, shallow water level and everywhere surrounded vegetation, all of which make data quality worse. Our test shows that in Amazon River nearly 60% of all waveforms are seriously polluted by the forest and valid land nearby, therefore, one particular phenomenon is for certain period of time, especially during the dry seasons (Winter), there is no qualified Topex data at all, even if there exists limited Topex data, it shows very low accuracy. Overall, accuracy of T/P in Amazon River decreased to 58 cm before retracking and 44 cm after retracking, which is half a meters level. Thus, for hydrologic purpose in small scale water bodies, especially for the use of monitoring water level change preciously, or calculate the volume of water resource, satellite altimetry seems not to be a good choice.

BIBLIOGRAPHY

Alsdorf, D., Birkett, C.M., and Dunne, T., 2001: Water level change in a large Amazon lake measured with space borne radar interferometry and altimetry.

Bamber, J., 1994: A new high resolution DEM of Greenland fully validated with airborne laser altimeter data. Journal of geophysical research, VOL.106, NO.B4, page 6733-6745.

Birkett, C.M., 1998: Contribution of the Topex NASA radar altimetry to the global monitoring of large rivers and wetlands.

Birkett, C.M., Mertes, L.A.K., Dunne, T., Costa, M.H., and Jasinski, M.J., 2001: Surface water dynamics in the Amazon Basin: Application of satellite radar altimetry, Doi: 10.1029/2001JD000609

Guo, J.Y., Gao, Y.G., Chang, X.T., Hwang, C.H., 2010: Optimized threshold algorithm of Envisat waveform retracking over coastal sea. Chinese Journal of geophysics Vol.53, No.2, 2010, page: 231-239

Guo, J.Y., Sun, J.L., Chang, X.T., Guo, S.Y., and Liu, X., 2009: Correlation Analysis of NINO3.4 SST and Inland Lake Level Variations Monitored with Satellite Altimetry: Case Studies of Lakes HongZe, Khanka, La-ang, Ulungur, Issyk-Kul and Baikal, doi: 10.3319/TAO.2010.09.17.01 (TibXS)

Hwang, C.W., Kao, Y.H., and Tangdamrongsub, 2010: A Preliminary Analysis of Lake Level and Water Storage Changes over Lakes Baikal and Balkhash from Satellite Altimetry and Gravimetry. Doi: 10.3319/TAO.2010.05.19.01(TibXS)

Hwang, C.W., Peng, M.F., Ning, J.S., and Sui, C.H., 2004: Lake level variations in China from TOPEX/Poseidon altimetry. Doi:10.1111/j.1365-246X.2005.02518.x

Ilce de Oliveira, C., Mercier, F., Maheua, C., Cochonneauc, G., and Kosuthc, P., 2001: Temporal variations of river basin waters from Topex/Poseidon satellite altimetry, application to the Amazon basin.

Lee, H.K., 2008: Radar Altimetry Methods for Solid Earth Geodynamic Studies.

Lee, H.K., Shum, C. K., Kuo, C.Y., Yi, Y.C., and Braun, A, 2006: Application of TOPEX Altimetry for Solid Earth deformation Studies. Doi: 10.3319/TAO.2008.19.1-2.37 (SA)

Lee, H.K., Shum, C. K., Tseng, K.H., Guo, J.Y., and Kuo, C.Y., 2010: Present-Day Lake Level Variation from Envisat Altimetry over the Northeastern Qinghai-Tibetan Plateau: Links with Precipitation and Temperature. Doi: 10.3319/TAO.2010.08.09.01 (TibXS)

Le Provost, C., 2001: Ocean tides, Satellite altimetry and Earth sciences, L.L. Fu and A. Cazenave Ed., Academic Press.

Maheu, C., Cazenave, A., and Machos, C.R., 2003: Water level fluctuations in the Plata Basin (South American) from Topex satellite altimetry. Doi: 10.1029/2002GL016033

Seeber, G., 2003: Satellite Geodesy 2nd completely revised and extended edition.

Torge, W., 2001: Geodesy 3rd edition.

Vivien, E., 2007: A new way of using altimetry waveform data over continental waters.

Zhang, M.M., 2009: Satellite Radar Altimetry for Inland Hydrologic Studies.

Zwally, H.J., 1989: Mass changes of the Greenland and Antarctic ice sheets and shelves and contributions to sea-level rise: 1992–2002.

ACKNOWLEDGEMENT

This research is conducted under the supervision of Prof. Nico Sneeuw and M.Sc. Mohammad J. Tourian of Stuttgart University, and I would like to take this opportunity to express my sincere gratitude to them for their professional guidance, encouragement and support during my graduate studies.

The research results documented in this report resulted in a Master Degree Dissertation. NASA and CNES provide the TOPEX/POSEIDON data products.